REPUBLIC OF TURKEY
ADANA ALPARSLAN TÜRKEŞ SCIENCE AND TECHNOLOGY UNIVERSITY

INSTITUTE OF GRADUATE SCHOOL
DEPARTMENT OF MATERIALS ENGINEERING

HALLOYSITE NANOTUBES REINFORCED POLYBUTYLENE TEREPHTHALATE BASED NANOCOMPOSITES: MECHANICAL, THERMAL, STRUCTURAL AND MORPHOLOGICAL CHARACTERIZATIONS

MUSTAFA ŞENYEL
MASTER OF SCIENCE

ADANA 2022

REPUBLIC OF TURKEY
ADANA ALPARSLAN TÜRKEŞ SCIENCE AND TECHNOLOGY UNIVERSITY

INSTITUTE OF GRADUATE SCHOOL
DEPARTMENT OF MATERIALS ENGINEERING

HALLOYSITE NANOTUBES REINFORCED POLYBUTYLENE TEREPHTHALATE BASED NANOCOMPOSITES: MECHANICAL, THERMAL, STRUCTURAL AND MORPHOLOGICAL CHARACTERIZATIONS

MUSTAFA ŞENYEL
MASTER OF SCIENCE

SUPERVISOR
ASSOC. PROF. DR. ALİ SİNAN DİKE

ADANA 2022

HALLOYSITE NANOTUBES REINFORCED POLYBUTYLENE TEREPHTHALATE BASED NANOCOMPOSITES: MECHANICAL, THERMAL, STRUCTURAL AND MORPHOLOGICAL CHARACTERIZATIONS

Submitted by **Mustafa Şenyel** in partial fulfillment of the requirements for the degree of **Master of Science in Department of Materials Engineering, Adana Alparslan Türkeş Science and Technology University** by,

Assoc. Prof. Dr. Ahmet BEYCİOĞLU
Graduate School Director

Prof. Dr. Mustafa GÜNEŞ
Department Chair

Assoc. Prof. Dr. Ali Sinan DİKE
Supervisor

Thesis Committee

Assoc. Prof. Dr. Ali Sinan DİKE
Adana Alparslan Türkeş Science and Technology University

Prof. Dr. Mehmet DOĞAN
Erciyes University

Prof. Dr. Osman SİVRİKAYA
Adana Alparslan Türkeş Science and Technology University

Thesis Defense Date: 24/02/2022

I hereby declare that all information in this thesis has been obtained and presented in accordance with academic rules and ethical conduct. I also declare that, as required by these rules and conduct, I have fully cited and referenced all information that is not original to this work.

[Signature]

Mustafa ŞENYEL

ABSTRACT

HALLOYSITE NANOTUBES REINFORCED POLYBUTYLENE TEREPHTHALATE BASED NANOCOMPOSITES: MECHANICAL, THERMAL, STRUCTURAL AND MORPHOLOGICAL CHARACTERIZATIONS

Mustafa ŞENYEL

Department of Materials Engineering

Supervisor: Assoc. Prof. Dr. Ali Sinan DİKE

February 2022, 60 pages

Polybutylene terephthalate (PBT) nanocomposites were melt-blended with two types of Turkish halloysite nanotubes (HN) using a co-rotating twin-screw extruder. Naturally occurring HN samples were used to produce PBT-based composites at the HN compositions of 1%, 3%, 5%, and 10% by weight. PBT was purchased as bead form under the trade name of Advanite from Sasa polyester A.Ş., Adana, Turkey. Neat and silane-modified grade of HN was supplied by Eczacıbaşı Esan, İstanbul, Turkey with the trade names of ESH HNT and ESH HNT S, respectively. Test samples were prepared by an injection molding process. Mechanical, thermo-mechanical, thermal stability, melt-flow, structural and morphological properties of the produced nanocomposites were reported using tensile, impact and shore hardness tests, dynamic mechanical analysis (DMA), thermo-gravimetric analysis (TGA), melt flow rate and density measurements and scanning electron microscopy (SEM) methods, respectively. Results of neat and silane coated HN containing composite samples were compared in order to investigate the interfacial adhesion between polymer matrix and reinforcement material.

Keywords: poly (butylene terephthalate), nanocomposites, halloysite nanotube, polymer composites

ÖZET

HALLOYSİTE NANOTÜP İLE GÜÇLENDİRİLMİŞ POLİBÜTİLEN TEREFTALAT BAZLI NANOKOMPOZİTLERİN MEKANİK, ISISAL, YAPISAL VE MORFOLOLİK KARAKTERİZASYONLARI

Mustafa ŞENYEL
Malzeme Mühendisliği Anabilim Dalı
Danışman: Doç. Dr. Ali Sinan DİKE
Şubat 2022, 60 sayfa

Polibütilen tereftalat (PBT) nanokompozitler, birlikte dönen çift vidalı ekstrüder kullanılarak iki çeşit Türk halloysit nanotüp (HN) ile eritilerek harmanlanmıştır. Doğal olarak oluşan HN numuneleri, ağırlıkça %1, %3, %5 ve %10 HN bileşimlerinde PBT bazlı kompozitler üretmek için kullanılmıştır. PBT boncuk formunda, Advanit ticari adıyla Adana'da bulunan Sasa Polyester A.Ş.'den temin edilmiştir. Saf ve silan modifikasyonlu HN ise, ESH HNT ve ESH HNT S ticari adlarıyla İstanbul'da bulunan Eczacıbaşı Esan firmasından tedarik edilmiştir. Test numuneleri enjeksiyon kalıplama prosesi ile hazırlanmıştır. Üretilen nanokompozitlerin mekanik, termo-mekanik, termal kararlılık, eriyik akışı, yapısal ve morfolojik özellikleri sırasıyla çekme, darbe ve shore sertlik testleri, dinamik mekanik analiz (DMA), termo-gravimetrik analiz (TGA), erime akış hızı ve özkütle ölçümleri ve taramalı elektron mikroskobu (SEM) yöntemleri kullanılarak tayin edilmiştir. Polimer matris ve takviye malzemesi arasındaki ara yüzey yapışmasını araştırmak için saf ve silan kaplı HN içeren kompozit numunelerin sonuçları karşılaştırılmıştır.

Anahtar Kelimeler: poli (bütilen terefitalat), nanokompozitler, halloysite nanotüp, polimer kompozitler

Dedicated to my family

ACKNOWLEDGEMENTS

Firstly, I wish to express my deepest gratitude to my thesis advisor Assoc. Prof. Ali Sinan Dike for his kind guidance, support, criticism and valuable discussions during my thesis study. His approach to the students and solving the problems will surely help me in my future career.

I am also grateful to Asst. Prof. Dr. Ümit Tayfun from Bartin University for their valuable support and contributions to the development of composite samples on material fabrication, processing and characterization stages.

I would like to sincerely thank Dr. Alinda Öykü Akar from Esan Eczacıbaşı Ltd. for her help on supplying halloysite clay samples and conducting tests including thermal analysis, hardness, density measurements.

I wish to express my sincere thanks to Prof. Teoman Tinçer for providing me opportunity to use the instruments in METU polymer laboratory.

I wish to thank Assoc. Prof. Mehmet Kodal from Kocaeli University to use DMA instrument in his laboratory to provide thermo-mechanical test data.

Additionally, I would like to express my thanks to all administration and academic staff in the Department of Materials Engineering at Adana Alparslan Türkeş Science and Technology University for their help and cooperation. Also I would like to thank my colleague Barış Günay for valuable contributions. Finally, I would like to thank my company Güney Çelik A.Ş. for corroborating and providing opportunity for my academic progress.

I would like to dedicate this thesis to my family for being always right beside me.

TABLE OF CONTENTS

LIST OF FIGURES

LIST OF TABLES

NOMENCLATURE

PMNC	: Polymer Matrix Nanocomposite
DMA	: Dynamic Mecphanical Analysis
FTIR	: Fourier Transform Infrared Spectrometry
HNT	: Halloysite Nanotube
J	: Joule
MFR	: Melt Flow Rate
PE	: Polyethylene
PBT	: Poly (butylene terephthalate)
PLA	: Poly (lactic acid)
PMMA	: Poly (methyl methacrylate)
PP	: Polypropylene
PS	: Polystyrene
PTFE	: Poly (tetrafluoroethylene)
SEM	: Scanning Electron Microscopy
TGA	: Thermal Gravimetric Analysis
T_g	: Glass Transition Temperature

1. INTRODUCTION

The nanocomposite material is made up of non-metallic, metallic, and polymeric components. A nanocomposite material is defined as a mixture of two materials, one of which is at least a nanometer scale. The nanostructure phases of a nanocomposite structure may be classified into four types; zero-dimensional (0D, embedded cluster), one dimensional (1D, nanotubes), two dimensional (2D, nanoscale plates) and three dimensional (3D, embedded network). Specific procedures can give some new characteristics and extra benefits to enhance the basic properties of a nanocomposite or to overcome a material deficiency. Nanocomposite materials have certain advantages and disadvantages (Bogue, 2011; Ebrahimi and Dabbagh, 2019).

The following are the primary advantages of nanocomposites over other composite materials:

- Small additive size and distance between additives thanks to high surface/volume ratio,
- Improved mechanical strength
- High ductility in absence of strength reduction
- Enhanced optical behaviors depends on the particle size

The disadvantages of using nanocomposite materials are as follows:

- Decrease in impact resistance toughness stems from the dispersion of nano-particles into bulk matrices,
- The limited data provide explanations regarding the structure-property relationship in the composite system (Viswanathan et al., 2006).

Despite numerous studies on the creation of nanocomposites that have been published, attaining homogenous dispersion of nanoparticles in polymeric matrix remains problematic. The Van der Waals attraction between nanoparticles favors the development of clusters and agglomerates in many circumstances. Furthermore, hydrophilic nanoparticles and hydrophobic polymers are incoherent, resulting in weak interfacial adhesion, poor dispersion, and poor characteristics. As a result, nanocomposites occasionally exhibited inferior characteristics to regular polymers, limiting their application range (Harito et al., 2019; Nazir et al., 2016).

to improve the qualities of nanocomposites, the nanosized particles must be properly spread and disseminated in the matrix material; otherwise, particle agglomeration will occur, and the properties of the nanocomposites would deteriorate (Camargo et al., 2009; Vinyas et al., 2019).

Nanocomposite materials may be produced using procedures comparable to those used for traditional polymer composites, making them particularly appealing from a manufacturing standpoint. They may also be made through in-situ synthesis of inorganic nanoparticles, which is known as hybrid polymer materials (Gerasin et al., 2013.)

1.1. Polymeric Composite Materials

Polymer nanocomposite materials are a type of material that results from the right combining of two or more nanoparticles or other nanosized particles using appropriate processes and a mix of polymer technology and nanotechnology.

Polymer materials provide advantages such as lightweight, high durability, ease of processing, corrosion resistance, ductility, and low cost. Polymers have inferior thermal, electrical, and mechanical qualities when compared to other materials such as ceramics and metals. Moreover, they have poor gas barrier qualities, heat resistance, and fire performance. Because polymers are less dense than ceramics and metals, they have various applications in industries such as automobiles, military, aircraft, and electronics. They, on the other hand, have a low coordination number and lightweight atoms of carbon and hydrogen as a backbone, which supports their usage as lightweight structural components and building materials (Paul and Robeson, 2008).

Polymer is the primary ingredient of polymer matrix nanocomposite. Polymers of various types are employed in the fabrication of polymer matrix nanocomposites. These polymers are detailed below:

1. Thermoplastics including commodity plastics and polyolefines,
2. Thermosetting polymers,
3. Elastomers,
4. Biodegradable and naturally derived polymers (Bharatiya et al., 2021).

According to research studies, nanoscale additions induce novel phenomena that affect material characteristics. Adding nanoparticles with a large surface area, anisotropic shape, and

high surface energy reduces the distance between interparticle in the polymer matrix. Furthermore, the nanoscale additions improve the strength of the polymer matrix connection. Because of this, polymer nanocomposites with totally new characteristics are suitable for new application areas (Silvestre et al., 2016).

1.1.1 Properties of Polymer Matrix Nanocomposites

Polymer nanocomposites have several unrivaled features, including biological capabilities, catalytic properties, electrochemical properties, mechanical properties, magnetic properties, and so on. Polymer nanocomposites have a wide range of possible applications due to their exceptional characteristics. Many researchers have reported on the fundamental and new uses of polymer nanocomposites. Polymer nanocomposites are categorized into two types based on the complexity and diversity of nanoscale units: inorganic and organic materials filled with polymer nanocomposites (Athimoolam and Moorthy, 2012).

The interaction between the polymer matrix and the nanofiller results in a molecular attraction effect between nanocomposites. The addition of a modest amount of nanofiller with dimensions less than 10 Å to the matrix, on the other hand, causes a change in the characteristics of the composite material. The nanocomposites production can be achieved by using the same methods that are applied for the typical composites such as in-situ, solvent method, or mixing melted polymer matrix. Nanocomposites can be created using the same processes as traditional composites, such as in-situ, solvent approach, or combining melted polymer matrix (Allegra et al., 2008; Hussain et al., 2006; Zeng et al., 2005).

Polymer matrix composites are the most extensively utilized composite materials due to their inherent characteristics. They have the following qualities when compared to conventional materials such as pottery. The combination of high-performance and low-density reinforcing fibers, resulting in relatively low modulus, generates polymer nanocomposites with high specific strength and modulus (Fu et al., 2019; Jancar et al., 2010; Mittal, 2009).

Because of the difference in cracking mechanisms, polymer matrix nanocomposites have a greater damage tolerance when compared to conventional materials. Matrix cracking, splitting or breaking fibers, and interfacial debonding are observed in polymeric nanocomposites,

whereas crack propagation causes fracture in typical materials. Since polymer nanocomposites have strong damping properties, it has a wide range of applications as a vibration absorption material (Utracki, 2004).

1.1.2 Application of Polymer Matrix Nanocomposites

The advancement in the characteristics of polymer nanocomposite materials has resulted in a plethora of industrial uses such as fuel tanks, packaging, power tool housing, solar cells, fuel cells, and plastic containers. Many polymer nanocomposites based on polymers have been marketed for gas barrier applications, ranging from butyl rubber to styrene-butadiene rubber (Bratovčić et al., 2015; Farhoodi, 2016).

Polymer nanocomposite is a material that is utilized in the optical glass and membrane industries. One of the most intriguing application areas is the manufacture of chemical protection and surgical gloves to guard against chemical agents and contamination from medicine. Polymers containing clay, for example, have demonstrated that they may improve the hardness and toughness of transparent materials without affecting their light transmission. In other words, they may be utilized to change the surface qualities of materials. According to certain studies, polymer nano coatings improve the durability, wettability, weather resistance, and abrasion resistance of material surfaces. Composites with changes in composition and structure on a nanometre scale have demonstrated impressive property gains over standard composites:

- Improved modulus,
- Enhanced gas barrier,
- Increase in heat distortion temperature,
- Optimized ablative resistance,
- Impact resistance retention.

Surprisingly, significant performance increases are accomplished without increasing the density of the basic polymer, diminishing its optical properties, or making it less recyclable (Manocha et al., 2006; Farhoodi, 2016).

1.2. Halloysite Nanotubes (HNTs)

Halloysite nanotubes (HNTs) are naturally occurring, harmless, and biocompatible tubular substances. Halloysite nanotubes feature a high aspect ratio, large pores, a non-swelling nature, and the capacity to regenerate. The composition of halloysite is made up of four elements: Al, Si, H, and O. HNTs is a fine clay mineral with a multilayered wall structure. The chemical formula of HNTs can be defined as $Al_2Si_2O_5(OH)_4$. nH_2O. HNT clays are naturally formed in the earth's crust over millions of years and are constituted of a double layer of aluminum, silicon, hydrogen, and oxygen (Massaro et al., 2020; Hillier et al., 2016).

HNTs are naturally found in many different parts of the world, including Turkey, Australia, United States, New Zealand, Brazil, France, and China. Halloysite is the most commonly found in weathered or hydrothermally altered rocks, saprolites, and soils. It can also be formed by the weathering, pedogenesis, or hydrothermal alteration of ultramafic rocks, volcanic glass, and pumice. The raw HNT is often mined from natural deposits, which occur widely in moist tropical and subtropical soils, and worn rocks, which are generated by the weathering of various types of igneous rocks. Because of structural and chemical similarities, HNT behaves similarly to kaolin clay. HNT occurs in a variety of morphologies, including platy, spheroidal, and tubular. Nonetheless, in the natural environment, the tubular structure is the predominant morphology of HNT during some popular procedures applied for treating industrial minerals including acid or alkaline treatment. Because of the high acid and alkaline conditions, both acid and alkaline treatment may disrupt the structure of HNT by causing dealumination and desilication (Joussein et al., 2005; Rawtani and Agrawal, 2012; Sagare et al., 2021; Yuan et al., 2015).

Ceramic raw materials, catalysts, adsorbents, electrical components, cosmetics and in-home and personal care goods, additives in polymers and plastics, and medication delivery vehicles are just a few of the commercial possibilities for HNTs. Furthermore, HNTs are being used as a template in nanotechnology. Because of their distinctive hollow architecture and huge cavity, HNTs are a suitable natural nano-carrier. The desirable interfacial affinity between the polymer and the Halloysite, as well as adequate Halloysite dispersion in the polymer matrix, are two important parameters for determining the performance of halloysite-polymer nanocomposites (Huang et al., 2016; Idumah et al., 2019; Liu et al., 2014).

When compared to other materials, HNTs offer several desirable properties, including a distinct micro-spatial structure, a large length-diameter ratio, a high lumen capacity, and chemical inertness. HNTs have a similar structure to carbon nanotubes (CNTs), but they offer several compelling advantages, including broadly spreadable performance, enhanced water solubility, stronger biocompatibility, and environmental friendliness (Erpek et al., 2017; Ezenkwa et al., 2022). HNT, on the other hand, cannot be distributed in polymer matrix due to the abundance of Al-OH groups, and their comparatively substantial surface energy associated with its large surface area induces agglomeration due to the existence of van der Waals interactions between tubes (Owoseni et al., 2015). Furthermore, significant shear stresses induced by techniques such as ball mill homogenization or melt extrusion to obtain fine and homogenous dispersion of HNTs in a polymeric matrix may avoid agglomeration of HNTs (Brantseva et al., 2018; Cheng et al., 2020; Doagou-Rad et al., 2020; Hope and Kittrick, 1964; Kausar, 2018).

In addition, to use several types of silane-coupling agents, a range of chemical groups such as epoxy, methacrylate, urea, and amine may be grafted on the surface of HNTs. Halloysite's electrophilic nature can be used to improve interfacial interactions in polymer composites (Cheng et al., 2018; Khunová et al., 2015; Lun et al., 2014). The common steps of silane modification process of HNT clay are visualized in Figure 1.1 (Kim et al., 2017).

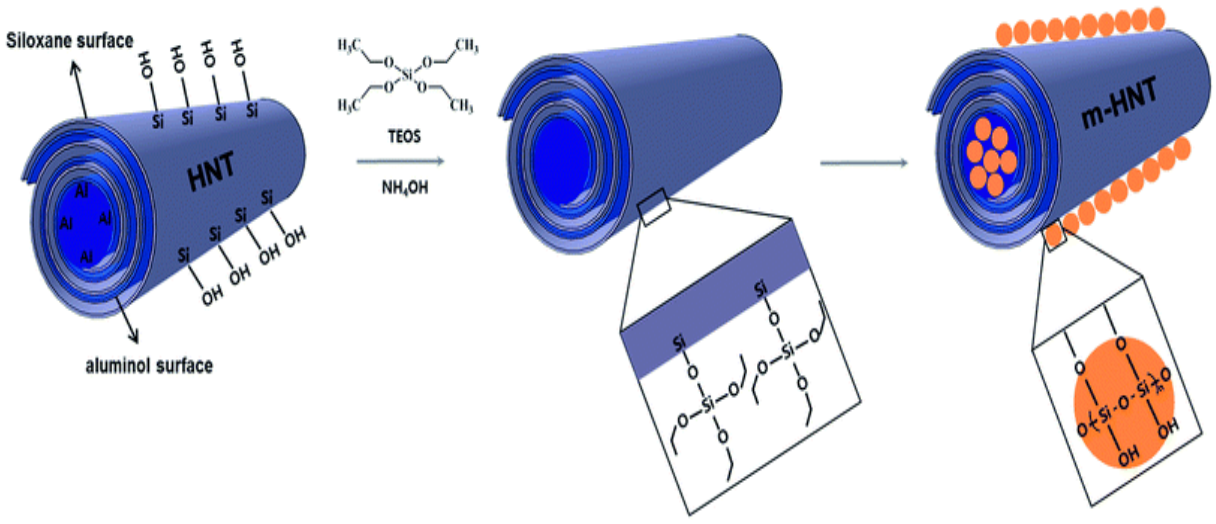

Figure 1.1 Schematic demonstration of HNT

1.3.Poly (butylene terephatalate) (PBT)

Poly butylene terephthalate (PBT) is a substantial, well-known commercially accessible semicrystalline engineering thermoplastic of the polyester family. It is produced by the polycondensation reaction of 1,4-butanediol with terephthalic acid (Van Berkel et al., 1997). Figure 1.2 demonstrates the chemical formula of PBT polymer.

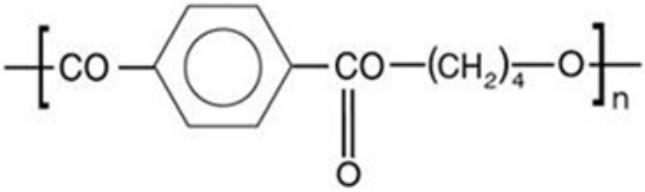

Figure 1.2 Schematic demonstration of PBT

PBT has a structure that is comparable to that of other aromatic polyesters like polyethylene terephthalate (PET) and poly trimethylene terephthalate (PTT). The structures of PET and PBT were compared in Figure 1.3 (Ito et al., 2008).

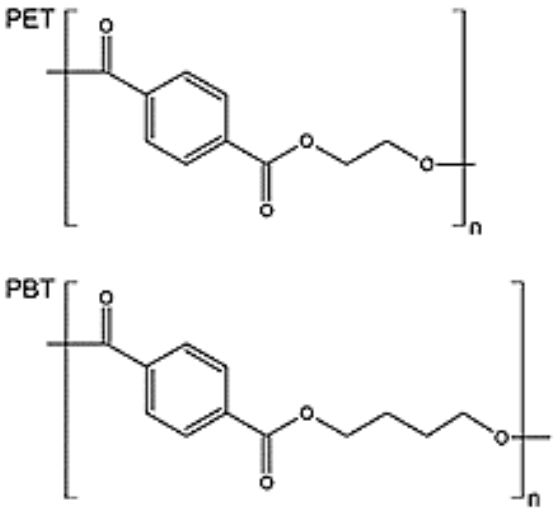

Figure 1.3 Schematic comparison of PBT and PET

PBT's overall behavior is similar to that of polyamides and PET. PBT is often recognized as polyamides' main competitor due to its superior physical properties, lower production costs, and great chemical resistance. On the other hand, it is widely acknowledged that PBT's high processability and exceptional properties make it simple to use in production lines (Bährle-Rapp, 2007; Deshmukh et al., 2011; McNally and Gall, 1986; Scheirs and Long, 2005).

PBT outperforms other polymeric materials in terms of water resistance, abrasion resistance, and solvent resistance, as well as mechanical strength, stiffness, and dimensional stability. PBT has a wide range of applications due to its remarkable qualities, including electric and electronic components, packaging, the automobile sector, notably vehicle parts in both under the hood and external applications, biomedical devices, and construction equipment (Correia Diogo, 2015; Park et al., 2010; Vilela et., 2014; Zhou et al., 2017).

In the automotive industry, PBT is commonly used as distributor caps, door handle components, and wheel covers. PBT is also utilized in the manufacture of circuit breakers, relays, connectors, and light sockets. The idea of using PBT as a nanofiller inside a polymer matrix and thereby modifying or boosting some properties of other polymers, on the other hand, has sparked the polymer industry's attention (Manuel and Gaymans, 1993; Patil et al., 2017; Ram, 1997).

1.4. Extrusion Process

When looking at the history of this extrusion, it appears that the operation was first used in the 1930s. The polymer extrusion melting method was first established in 1959. Extrusion is a continuous process that is capable of shearing, mixing, and transporting materials. This technique now produces more than half of all plastic items, including sheets, pipelines, and plastic bags (Cunha et al., 2009; Hyvärinen, 2020; Vergnes et al., 2001)

Extrusion is a very flexible technique that consists of several unit operations and is used to modify the physical characteristics of raw materials by forcing them through a die with the correct cross-section at elevated regulated pressure and temperature. Extrusion, in other terms, is the process of transforming raw material into a product of uniform shape and density by pushing it through a die under regulated conditions (Dogossy et al., 2013; Giles et al., 2005).

Extruders are typically made up of one or two screws and are housed in a barrel that is either grooved or smooth. The screw(s) is controlled by a motor, and the increment and decrease of screw speed is given by a gearbox during operation. Furthermore, there is a die at the end of the barrel, and the raw material that is pressed by the extruder is molded by the die (Lewandowski and Wilczyński, 2022).

Extruder equipment consists of monitoring devices for evaluating performance and quality, auxiliary equipment for the extruder, and downstream processing equipment. The basic components of an extruder include the die and screw driving mechanism, feeding hopper, single or twin screws, and barrels. The extruder's accessory equipment consists mostly of a solvent delivery pump, a heating/cooling device for the barrels, and a conveyor belt to dry the product. Temperature gauges, a screw-speed controller, an extrusion torque monitor, and pressure gauges are among the monitoring instruments on the equipment (Cheremisinoff, 1987; Wilczynski and White, 2003).

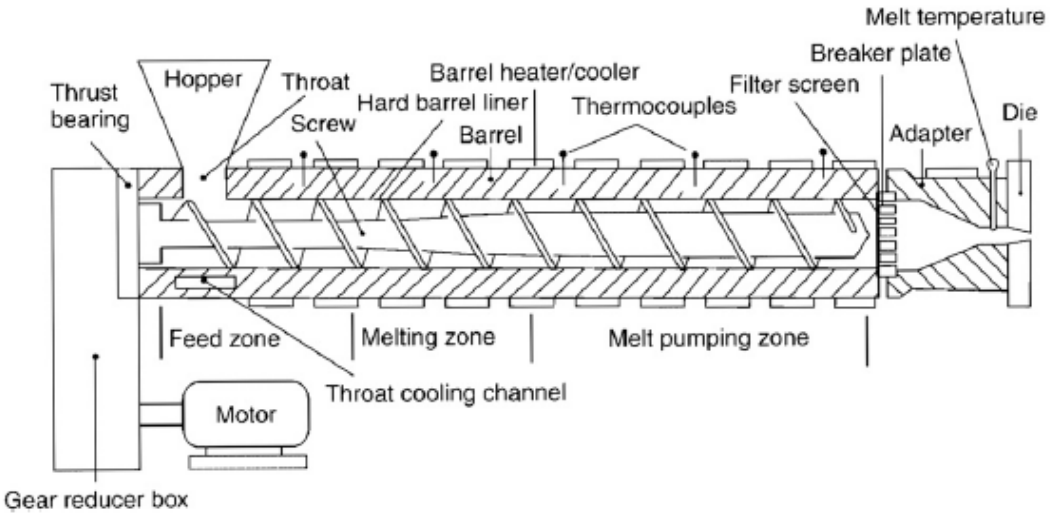

Figure 1.4 Cross-section of an extruder showing principal components

Processing of a polymer using extruder may be divided into eight separate sections as represented in Figure 1.4, which are;

1. Feeding stage
2. Plastication of polymer pellets
3. Conveying polymer
4. Mixing zone
5. Downstream feeding
6. Devolatilization of plastic
7. Pumping of polymer melt
8. The exit of the polymer through die

In comparison to other fabrication methods extrusion provides several advantages such as;

1. The reaction is carried out in the melt without the use of any solvents or chemicals.
2. Extruders can operate with highly viscous materials, while batch reactors cannot.
3. Modular geometry, high temperature, and mixing conditions are more adaptable than other processes.
4. Low-cost process with shorter manufacturing time and fewer processing stages
5. Constant operation
6. Excellent blending (uniform dispersion of nanofillers).

However, extrusion, like other manufacturing techniques, has inherent drawbacks including;

1. The substantial energy consumption since melt extruders require strong shear forces and relatively high temperatures,
2. The reaction management is problematic due to the extruder's limited cooling capacity in the case of very exothermic reactions,
3. Because the residence period of the raw material is restricted for this process, slow reactions are not achievable, even if the temperature and concentration of the reagents are regulated (Lafleur and Vergnes, 2014; Rubin, 1990).

1.5. Injection Molding Process

Injection molding is a crucial industrial process for making plastic items and parts. This approach requires an injection molding machine with a control unit, a suitably clamped mold with a cavity or cavities that specify the component shape, and, lastly, a mold temperature unit.

The procedure begins with the injection molding machine's hopper being filled with plastic pellets ranging in size from 2 to 3 mm. Whole pellets should be dried and moisture eliminated before feeding the machine (Fu et al., 2020; Kohlgrüber, 2012; Wood and Ullman, 1996). The basic items of an injection molding machine are shown in Figure 1.5.

In 1872, the first injection molding machine was notified and patented in the United States, and it was utilized exclusively for Celluloid. This machine's origins may be traced back to the pressure die casting process for metals. In the past, injection moulding machines were plunger-based but more dependable screw-based machines have become more popular in recent years (Chabot and Malloy, 1997; Isayev, 2000; Rosato and Rosato, 2012).

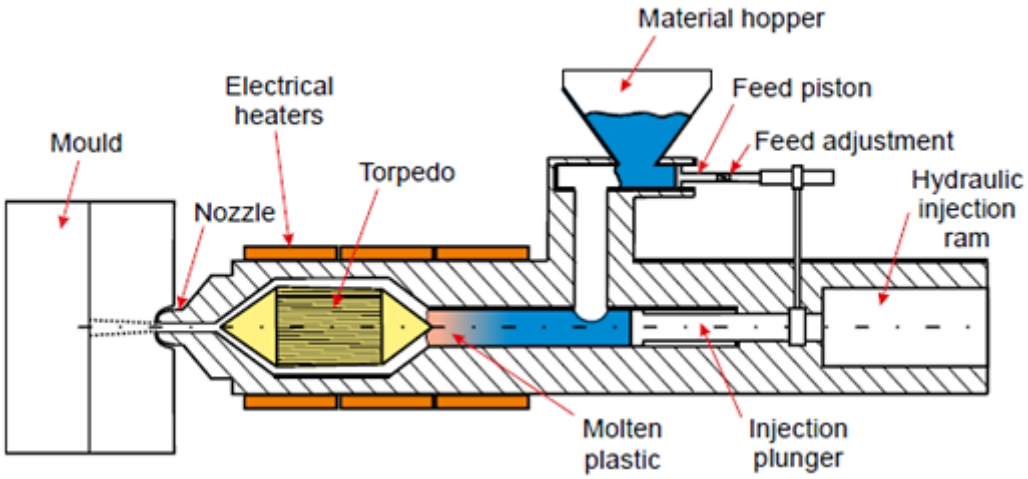

Figure 1.5 Cross-section of an injection molding instrument

1.5.1 Injection Molding Machinery

Even though injection molding machines come in a variety of shapes and sizes, they all perform the same basic activities. The basic procedure is the same for all of them. First, the material is melted or plasticized, then injected into the mold, which is then closed and the injected material is cooled. The conventional injection molding machine is made up of two basic units: the injection unit and the clamp unit. The injection unit's primary function is to evenly heat plastic material and inject it into the mold under predetermined circumstances such as pressure, flow rate, and so on. The clamp unit, on the other hand, is the second important portion of the machine that opens and closes the mold and holds the mold during injection of the polymer melt (Belofsky, 1995; Chval et al., 2020; Saurabh et al., 2020; Yen, 1996).

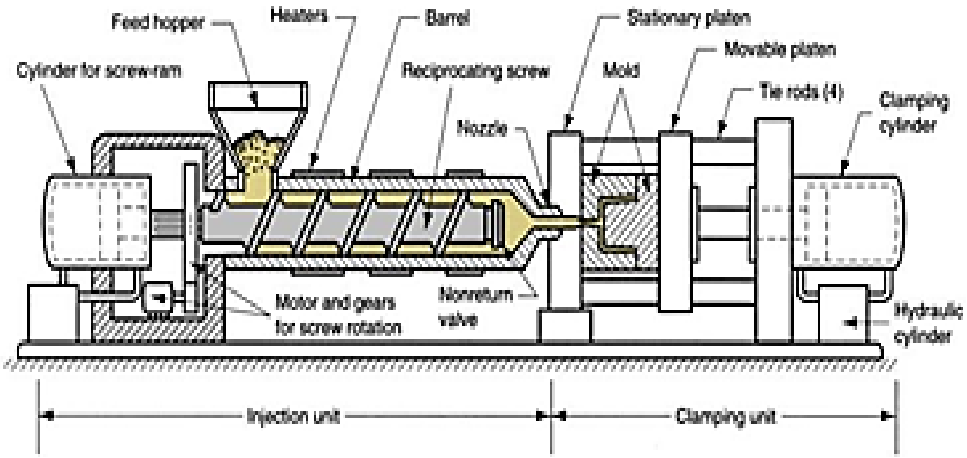

Figure 1.6 Two fundamental units of Injection Molding Machine

The procedure of injection molding is relatively straightforward. Pressure flow and heat transfer are the underlying mechanics of this process. First, the plastic material is heated until it melts, and then it is pressed into a closed mold that describes the shape of the finished product. Finally, the material is cooled until it returns to a solid-state, at which point the mold is opened and the finished object is expelled. Even if the technique is simple, the practice is not owing to the complicated behavior of plastic melts and complex results (Altan et al., 1993; Kent, 2006; Speranza et al., 2011). The representative illustration in Figure 1.6 indicates the injection unit and clamping unit of an injection molding machine during processing.

2. LITERATURE REVIEW

2.1. HNT reinforced polymer composites

Because of their nanoscale dimension and high aspect ratio, halloysite nanotubes are an excellent filler for a variety of polymers. Furthermore, halloysite nanotubes can improve a variety of polymer characteristics such as modulus, strength, stiffness, impact resistance, and mechanical performance of polymers at higher temperatures under both static and dynamic situations. In the high temperature range of 900-1000 °C, halloysite shows exothermic action. This thermal event is thought to be caused by the creation of a separate alumina-rich phase and amorphous silica. Some studies show that traces of iron in halloysite improve composite inflammation resistance, and it may also be used as a flame-resistant material in varied polymers (Duce et al., 2015; Goda et al., 2018; Jasinski et al., 2021; Jing et al., 2021; Wu et al., 2022).

HNTs can be intercalated with salts and organic compounds; this behavior has been thoroughly reviewed by Joussein et al. In contrast to organoclays, HNTs did not need to be intercalated before adding them to polymers because HNTs have a tubular microstructure and good dispersion (Joussein et al., 2005). Therefore, few works have focused on improving the effects of HNTs on polymers using intercalation (Khunova et al., 2013).

In a recent study, Akar et al. fabricated polyamide (PA) nanocomposites involving amino-silane modified HNT (Akar et al., 2022). According to the results they obtained, low content (1% by weight) of HNT additions yielded improvements in dynamic mechanical, thermal, tensile and impact performances of composites. In their other publication, they conducted comprehensive research in which polyhedral oligomeric silsesquioxane (POSS) and HNT nano-additives were incorporated with thermoplastic polyurethane matrix both separately and hybrid forms (Mohamed et al., 2020). Their findings revealed that polyurethane nano-composite samples containing HNT with a concentration of 1% by weight exhibited optimum performance among prepared formulations. Additionally, HNT loadings led to an increase in melt-flow rates of composites which were associated with the high aspect ratio of halloysite clay.

Accordingly, the relationship between adding amount of HNT and property enhancements for its unsaturated polyester-based composites was examined by Kim et al. They reported that 1% wt content of HNT displayed superior performances in terms of mechanical properties (Kim et al., 2017). Their result based on the adding content was found to be in correlation with previously discussed studies published by Akar et al. (2022) and Mohamed et al. (2020).

Biodegradable poly (lactic acid) was compounded with HNT and produced composites were investigated by several research groups. For HNT containing PLA-based composites, it was found that strength, modulus, and toughness values were improved with the inclusion of HNT clay (Ertas et al., 2019; Prashantha et al., 2013). Adding a small amount of HNTs to PLA matrix led to an increase in crystallization rate, shorten the processing time and improve the heat resistance of the fabricated nanocomposites (Liu et al., 2013).

During melt-mixing of HNTs-polymer nanocomposite, the polymer chains can interact with the HNTs due to the strong shear force, leading to interfacial compatibility. The surface treatment of HNT can improve the interfacial interaction with polypropylene (Liu et al., 2008) and polyamide (Guo et al., 2009) matrices during melt processing.

Jia et al. reported the effects of HNT on flame resistance of low-density poly ethylene (LDPE). According to their cone calorimetric data, HNT inclusions showed a decrease in the flammability of LDPE significantly (Jia et al., 2009).

Halloysite inclusions donated varied property improvements including antioxidant resistance and oxygen barrier behaviors in packaging, film, and bottling application fields in which polyethylene (Garcia-Escobar et al., 2021), poly vinyl alcohol (Abdullah and Dong, 2020), poly lactide (Erpek et al., 2016; Tham et al., 2016), and oxidized starch (Abdullah and Dong, 2018; Kong et al., 2011) were loaded with HNT clay.

Based on the literature survey, only one study was published related to PBT composites filled with HNT clay performed by Oburoğlu et al. in which the influence of HNT additions to the crystallization kinetics of PBT chains was examined by differential scanning calorimeter (DSC) analysis data (Oburoğlu et al., 2012).

2.2. The novelty and aim of the study

This thesis study is primarily focused on the enhancement of basic properties of PBT with the help of the incorporation of HNT clay. The effects of modification of HNT were also examined to observe the interactions between HNT and PBT matrix through the mechanical, thermal, thermo-mechanical, melt-flow, and morphological performance of composite samples. Research data of composites containing neat HNT clay and silane-modified HNT were compared according to characterized behaviors. Additionally, additions of pristine and modified HNT into PBT matrix were investigated individually for different concentrations.

A different aspect of the study than the previously published ones is the performance evaluation of PBT/HNT nanocomposite system. As indicated in the literature review previously, one research study was found dealing with HNT reinforced PBT composites published by Oburoğlu et al. (2012) in which thermal crystallization behavior of PBT in presence of HNT using DSC analysis. This thesis study is different from that research work according to the characterization steps including mechanical, physical, thermo-mechanical, and morphological analyzes in addition to comprehensive discussions based on the pristine and silane-modified grades and adding ratios of both HNT clays. Accordingly, the investigation of silane modification of HNT on the basic properties of PBT/HNT nanocomposite system makes this research a novel experimental study.

Conventional processing techniques of PBT-based nanocomposites were applied for the aim of their cost-effectiveness, practical applications, and the compatible adaptation of scale-up characteristics.

3. MATERIALS AND METHODS

3.1. Materials

3.1.1. Poly (buthylene terephthalate)

The commercial PBT thermoplastic polymer was purchased from Sasa Polyester Sanayi A.Ş., Adana, Turkey as a bead form. The trade name of PBT is Advanite. It has a viscosity of 0,90 dL/g according to the producer. The photograph of PBT pellets used in this thesis is shared in Figure 3.1.

Figure 3.1 The photograph of PBT beads used in this study

3.1.2. Halloysite Nanotubes

HN powders used in thesis study were supplied from Esan Eczacıbaşı Endüstriyel Hammaddeler Sanayi ve Ticaret A.Ş., İstanbul, Turkey. The photograph of HN grades used in this thesis is shown in Figure 3.2.

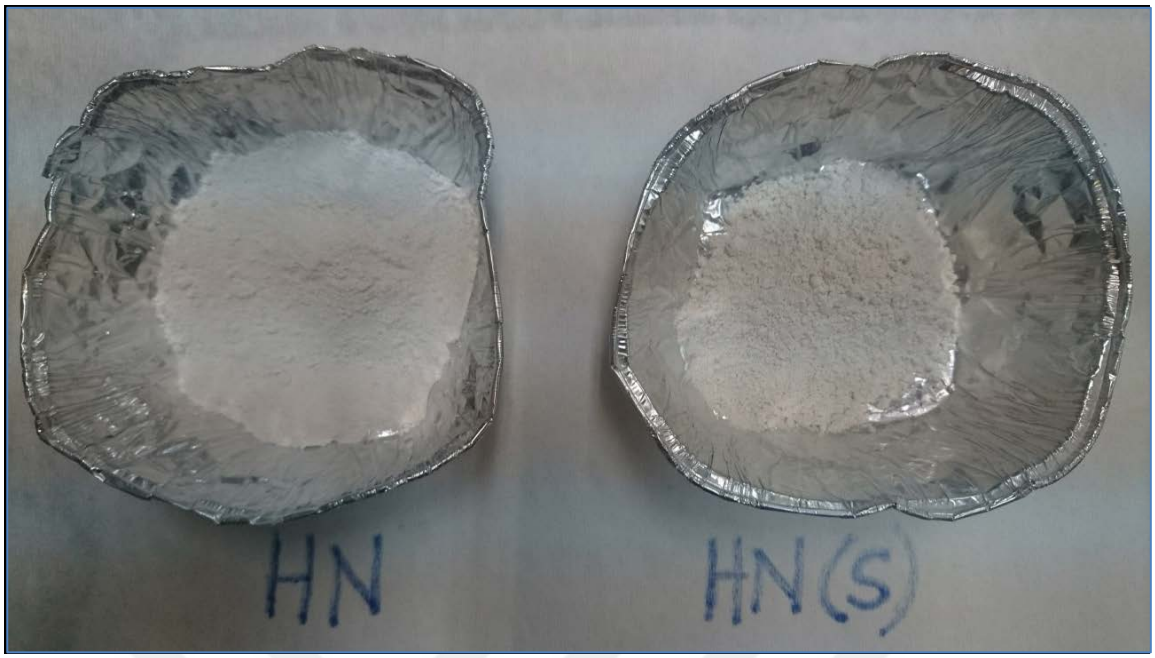

Figure 3.2 The photograph of HN samples used in this study

As can be seen in Figure 3.2, two kinds of HN grades were used with the commercial names of ESH HNT (HN) and ESH HNT S (HN-S) which stood for unmodified and silane-modified grades, respectively. The basic physical properties of HN grades provided by the producer are listed in Table 3.1.

Table3.1 Properties of HN used in this study

Specification	**Value**
Lightness-Darkness (L)	96.81
Brightness (ISO)	84.47
Whiteness (CIE)	2.75
Refraction Index	1.55
Specific Gravity	2.75
Bulk Density (g/cm^3)	0.56
Moisture Content (%)	0.14
Oil Absorption (g/100 g)	30.0

3.2. Production of composites

PBT pellets and HN powders were subjected to the drying stage at 100°C in an oven for 2 hours to avoid moisture contamination before processing steps. Polymer and powders were compounded by a lab-scale micro-compounder (MC 15 HT, Xplore Instrument Netherland) located in METU Polymer Lab as shared in Figure 3.3. Filling ratios of NC 130 and NC 140 into PBT matrix were set as 1, 3, 5, and 10 by weight % as indicated in Table 3.2.

Table3.2 Compositions of prepared composites

Sample Names	**PBT composition (wt%)**	**HN composition (wt%)**	**HN-S composition (wt%)**
PBT	100	0	0
PBT/1 HN	99	1	0
PBT/3 HN	97	3	0
PBT/5 HN	95	5	0
PBT/10 HN	90	10	0
PBT/1 HN-S	99	0	1
PBT/3 HN-S	97	0	3
PBT/5 HN-S	95	0	5
PBT/10 HN-S	90	0	10

During the compounding process, extrusion temperature of 240˚C, mixing rate of 100 rpm and the total compounding time of 5 minutes were applied and these parameters were kept constant for each composite sample.

Figure 3.3 The lab-scale micro-compounder

Composite samples were cut to pellet form after the melt-compounding step. Samples were injection molded and dogbone specimens were obtained using a lab-scale micro-injection molding device (Micro-injector, Daca Instruments). The representative photographs of the micro-injector device which is located at METU Polymer Lab are shown in Figure 3.4. The dimensions of standard dogbone specimens were 80×7.5×2.5 mm^3. Processing parameters of injection molding were applied as barrel temperature of 245˚C, injection pressure of 800 kPa, holding time of 4 min and the mold temperature of and 80 ˚C.

Figure 3.4 The photograph of the micro-injector

3.3. Characterization Techniques

3.3.1. FTIR Spectroscopy

The characterization of surface properties of pristine and modified HN samples were performed by Shimadzu IRAffinity-1S FTIR Spectrometer in Bartin University Central Laboratory as can be seen from Figure 3.5. Analysis was carried out using attenuated total reflection (ATR) mode in the wavelength range of 4000–500 cm^{-1}.

Figure 3.5 The photograph of FTIR spectrometer

3.3.2. Tensile tests

Lloyd LR30K universal tensile testing equipment (Figure 3.6) in METU Polymer Lab was conducted to perform tensile tests. 5 kN load cell and 10 mm/min were applied as crosshead speed according to the standard of ASTM D-638. Tensile strength, percentage strain, and tensile modulus values were recorded by a minimum of three samples with standard deviations.

Figure 3.6 The photograph of the tensile testing device

3.3.3. Impact tests

Impact energy values of PBT and its composite samples were recorded by Coesfeld material impact tester in METU Polymer Lab with the 4 J pendulum in accordance with ASTM D256 standard procedure. The impact strength values in the unit of kJ/m^2 were expressed from measured impact energy data in the unit of J. The photograph of the impact tester used in this thesis work is displayed in Figure 3.7.

Figure 3.7 The photograph of impact tester device used in this study

3.3.4. Hardness tests

Shore D type hardness values of test samples with the dimensions of 20 x 20 x 2.5 mm^3 were recorded using a digital hardness device with the trade name of R5LB041, Zwick Roell as exhibited in Figure 3.8. Hardness measurements were done according to ISO 7619-1 standard.

Figure 3.8 The representative photograph of hardness tester device

3.3.5. Thermal gravimetric analysis

TGA analysis was carried out using Perkin Elmer Diamond TG/DTA device located in Esan R&D Lab with the heating rate of 10ºC/min and under the inert nitrogen atmosphere with the flow rate of 50 ml/min in a temperature range of 25-650ºC. Figure 3.9 displays the representative photograph of TGA device used in thermal studies.

Figure 3.9 The representative image of TGA thermal analyzer

3.3.6. Dynamic mechanical analysis

Thermo-mechanical behavior of PBT-based nano-composites was examined by dynamic mechanical analysis in dual cantilever bending mode. DMA tests of PBT and composite samples with the dimensions of 50×7.5×2.5 mm^3 were studied using Hitachi High-Technologies, Dynamic Mechanical Analyzer DMA7100 in Kocaeli University Polymer Lab. The temperature range of analysis was applied between 25°C and 200°C at the constant heating rate of 10°C/min under the inert nitrogen atmosphere. DMA analyzer equipment used in this research was demonstrated in Figure 3.10.

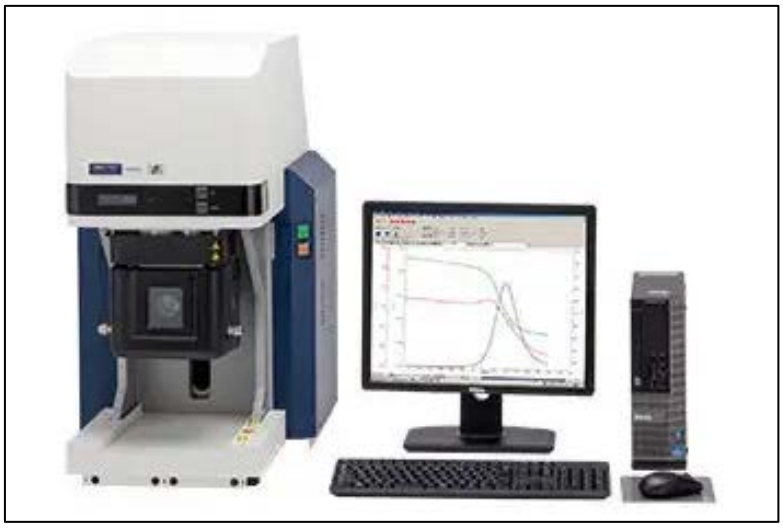

Figure 3.10 The representative image of dynamic mechanical analyzer

3.3.7. Melt flow rate measurement

MFR values of PBT and composite samples were evaluated using Meltfixer LT (Coesfeld Material Test) in METU Polymer Lab. The measurements were conducted by the standard load of 2.16 kg at the processing temperature of 240 °C. The MFR parameters were calculated and expressed in the unit of g/10 min. The photograph of Meltfixer device used in this study is represented in Figure 3.11.

Figure 3.11 The photograph of melt flow rate device

3.3.8. Density Measurements

The digital density-meter (Easy D30, Mettler Toledo) was utilized in ESAN R&D Lab as shown in Figure 3.12 to obtain density values of unfilled PBT and relevant composite samples. Density data was reported as an average of minimum of three measurements for each sample.

Figure 3.12 The photograph of density apparatus

3.3.9. Scanning Electron Microscopy

The fractured surfaces of composites samples obtained from the impact test were examined after coating a thin layer of gold. FEI Quanta 400F FESEM device was used to capture high-resolution SEM micro-images with the magnifications of x1,000, x2,500, x5,000 and x10,000. Figure 3.13 represents the sample holder equipment and microscope apparatus of SEM device used in this study.

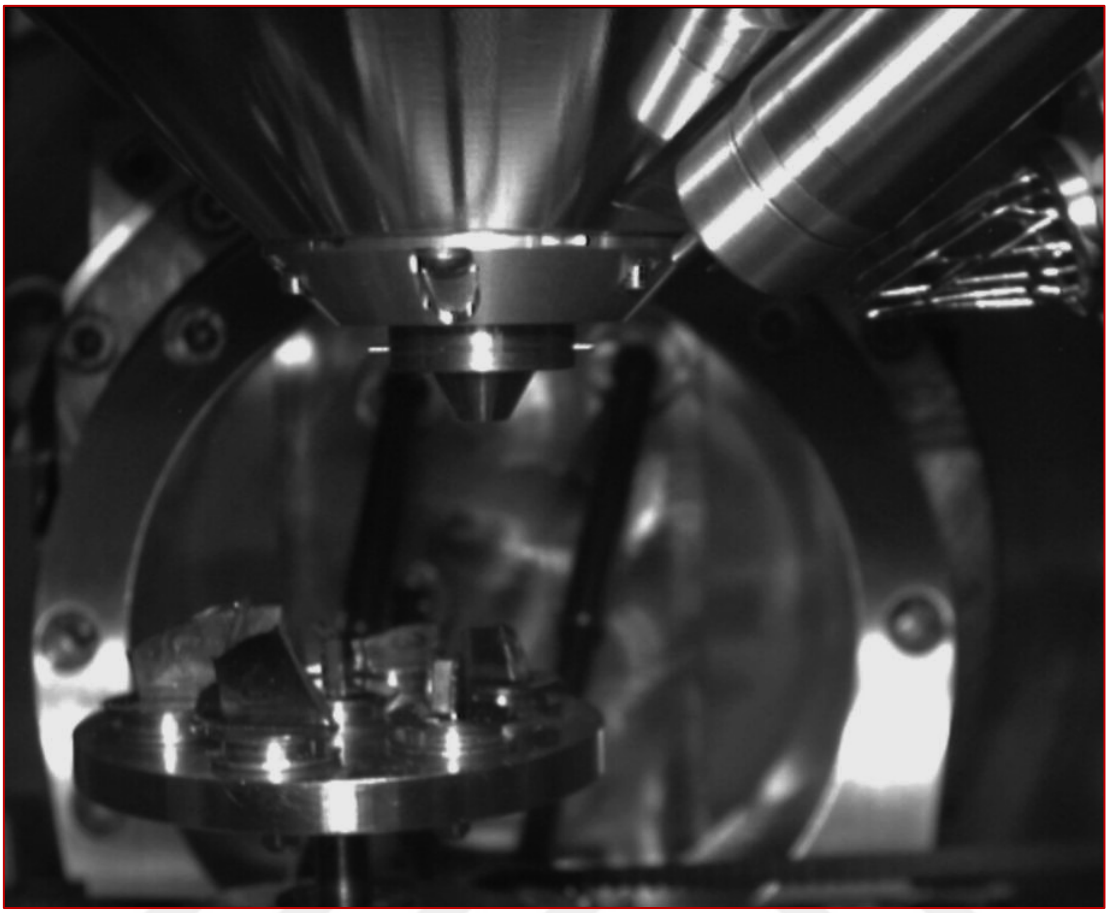

Figure 3.13 The microscope and sample holder of SEM apparatus

4. RESULTS AND DISCUSSIONS

4.1. FTIR Analysis of HN Powders

FTIR spectra of HN and HN-S surfaces are visualized in Figure 4.1.

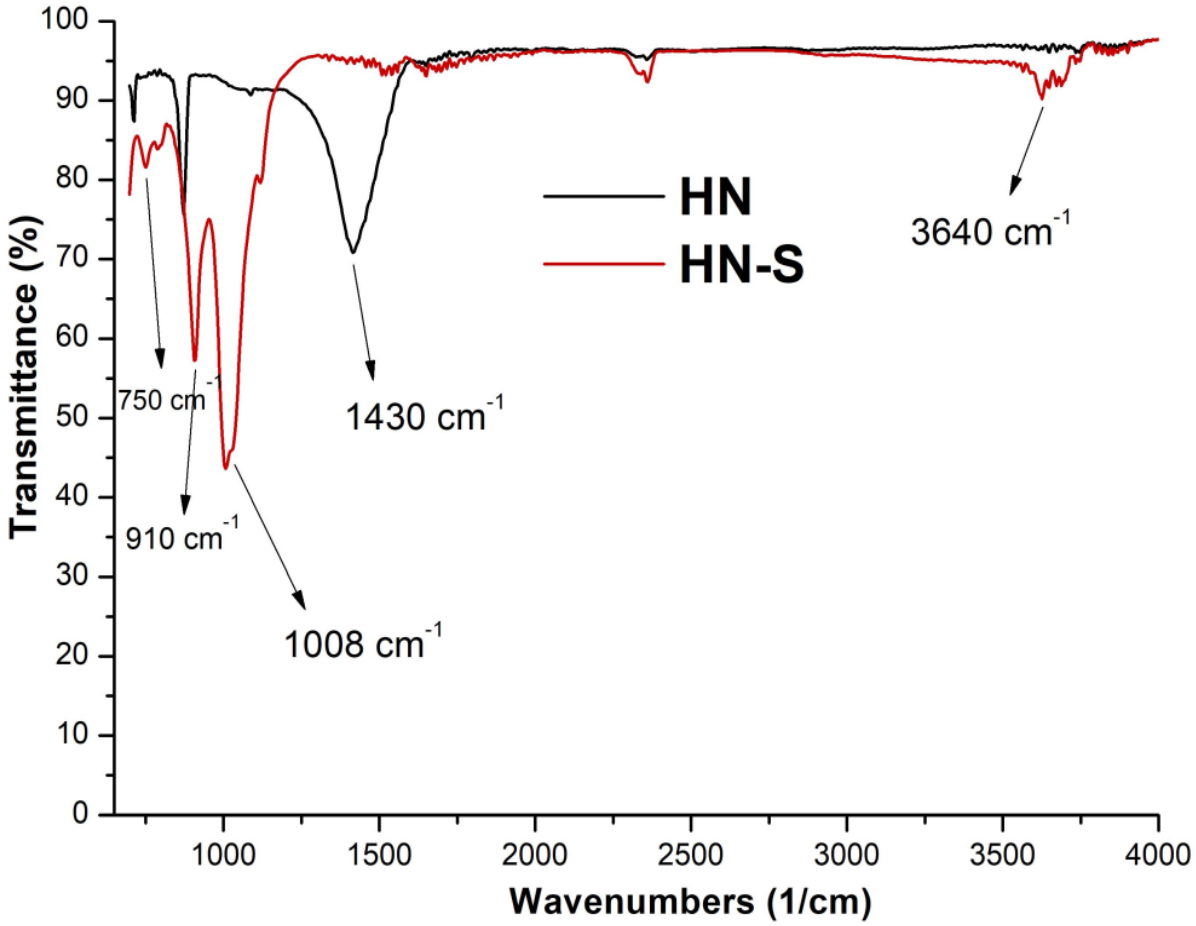

Figure 4.1 FTIR spectra of HN and HN-S powders

The main difference of two spectra was obtained as a broad band at 1430 cm^{-1} which was attributed to presence of zeolitic water on HN surface. This water related peak was found to be disappear after modification (Arat and Uyanık, 2017). The characteristic silicon related strong peaks observed at 1008, 910, and 750 cm^{-1} wavenumbers were assigned to Si-O stretching, Si-H bending and Si-O bending vibrations, respectively (Moazeni et al., 2015; Pal et al., 2014; Yildirimkaraman et al., 2020). Absorption peak located nearly at 3640 ascribed to stretching vibrations of hydroxyl group on HN-S surface.

4.2. Tensile Behaviours

Mechanical test data of PBT and its composites are listed in Table 4.1 and the stress versus percentage strain curves are given in Figure 4.2.

Table 4.1 Tensile test data of PBT and composites

Samples	**Tensile Strength (MPa)**	**Tensile Modulus (GPa)**	**Strain at Break (%)**
PBT	33.7±0.7	0.64±0.3	9.2±0.5
PBT/1 HN	34.2±0.5	0.67±0.2	8.4±0.6
PBT/3 HN	35.4±0.3	0.66±0.1	8.0±0.4
PBT/5 HN	35.1±0.3	0.77±0.1	8.6±0.5
PBT/10 HN	34.6±0.4	0.73±0.1	7.9±0.3
PBT/1 HN-S	43.4±0.3	0.75±0.2	9.3±0.4
PBT/3 HN-S	44.8±0.4	0.77±0.1	10.4±0.5
PBT/5 HN-S	43.9±0.2	0.73±0.1	11.3±0.3
PBT/10 HN-S	41.0±0.3	0.76±0.2	10.5±0.3

Based on the tensile test data in Table 4.1, tensile strength of neat PBT was found to be increased by HN additions. However, silane-modified HN inclusions yielded remarkably higher tensile strength values compared to unmodified HN. The amount of increment in tensile strength of PBT with the addition of pristine HN was obtained as a very low level. For example, PBT/3 HN gave a 5% increase in tensile strength of PBT. On the other hand, the degree of improvement in tensile strength was found to be relatively higher for HN-S containing composites in which approximately 30% increase in strength value was obtained for PBT/3 HN-S candidate with respect to unfilled PBT. In the case of adding amounts of HN and HN-S, tensile strength exhibited increasing up to 3% content by the inclusion of both additives. Their further loadings caused dramatic reductions which indicated that more than 3% adding ratios of halloysite showed a negative effect on tensile strength of composites. Composites reinforced with 3% of HN and HN-S displayed the greatest strength values.

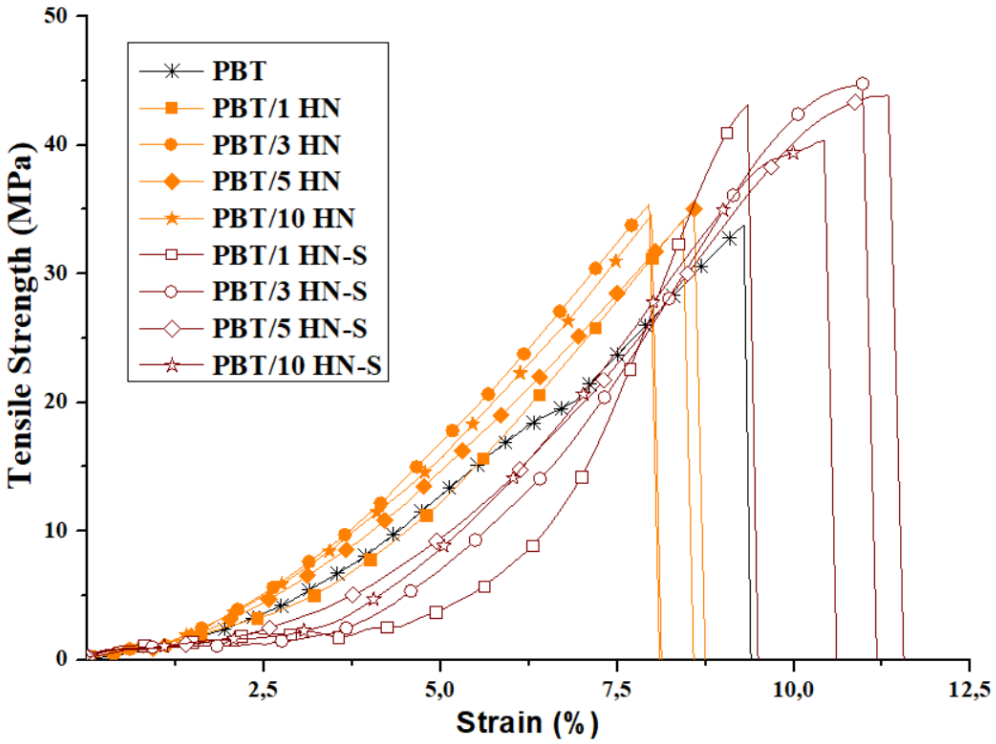

Figure 4.2 Stress versus strain curves of PBT and composites

The difference between tensile behaviors of composites loaded with modified and unmodified HNT can easily be observed from their tensile curves in Figure 4.2. The characteristic stress versus strain curve of PBT was started to give a necking behavior by the additions of HN-S. The necking observation in stress versus strain curves is linked to the tendency of a brittle polymer turned into a ductile characteristic. In other words, HN-S promoted ductility by reducing the brittleness of PBT phase. The absence of necking in tensile curves of PBT and unmodified HN containing PBT composites proposed that HN had no effect on brittle structure of PBT matrix.

According to tensile modulus data listed in Table 4.1, both additions of HN and HN-S resulted in increase for modulus of PBT. PBT/HN-S samples were found to be higher in terms of tensile modulus compared to PBT/HN for lower adding ratios, whereas, nearly identical modulus values were reached for their higher contents.

Strain at break values of neat PBT gave completely different trends by the additions of modified and unmodified HN as can be observed in Table 4.1. HN-S inclusions led to an increase in strain of PBT and the improvement carried on up to %5 concentration of HN-S.

On the contrary, composites involving unmodified HN yielded a drop-down in percentage strain of PBT. Strain values of composites reduced as the HN content increased. Relatively weak interactions between inert HN surface and PBT than that of silane-modified HN and PBT may be the main reason for the lowering of strain at break values.

According to the literature, in the case of HNT clay inclusion with 1% content, the highest level of mechanical behaviors was achieved (Akar et al., 2022; Kim et al., 2017; Velmurugan and Mohan, 2004). as similar to mechanical test data previously reported in this study.

4.3. Hardness Test

Shore hardness test data of PBT and its composites are listed in Table 4.2.

Table 4.2 Shore D hardness test data of PBT and composites

Additive/Content	**0 (PBT)**	**1%**	**3%**	**5%**	**10%**
HN	75.0±0.1	75.2±0.1	75.5±0.1	75.9±0.1	76.7±0.2
HN-S	75.0±0.1	75.3±0.1	75.7±0.1	76.1±0.2	77.0±0.2

The hardness of unfilled PBT was improved with halloysite inclusions. Silane-modified HN exhibited slightly higher hardness values compared to unmodified HN. Shore D hardness of composites was enhanced as the filling amounts of HN and HN-S increased. The overall change in Shore D hardness parameter of PBT was found to be in a narrow range after HN additions regardless of the types of HN grades.

4.4. Impact Performances

Impact strength results of PBT/HN and PBT/HN-S composite samples are demonstrated as bar graphs in Figure 4.3 and Figure 4.4, respectively. Additionally, impact strength values of each sample were indicated above its bar graph.

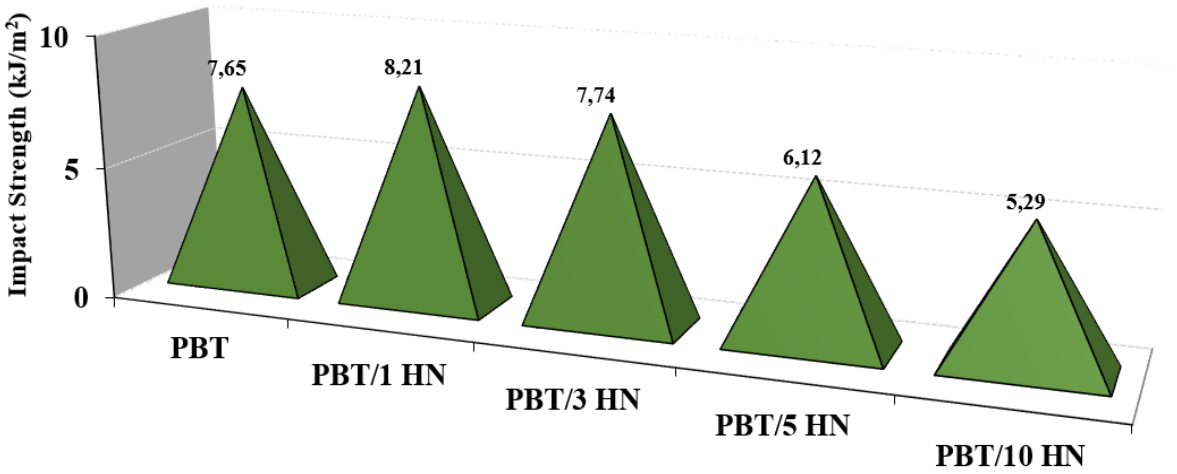

Figure 4.3 Impact test results of PBT/HN composites

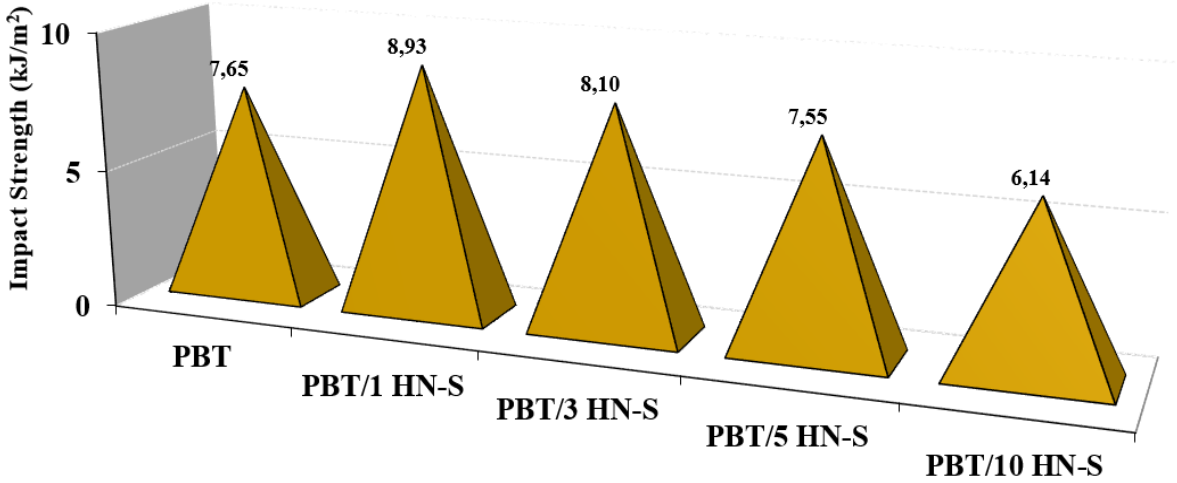

Figure 4.4 Impact test results of PBT/HN-S composites

According to Figure 4.3 and Figure 4.4, HN and HN-S inclusions with low contents (1% and 3%) resulted in enhancements for impact performance of neat PBT. However, high loading amounts of both HN grades reduced the impact energy of composites. Silane-modified HN reinforced PBT yielded slightly higher impact energy values compared to composites containing unmodified HN clay which may be attributed to stronger interfacial adhesion of HN-S to PBT with respect to neat HN. The related weak bonding through HN-PBT interphase resulted in a decrease in resistance against impact deformation. Based on these findings, it can be said that halloysite clay can be act as an impact modifier for PBT with its low loading ratios (Akar et al., 2021; Baxi et al., 2011; Beake et al., 2004; Hage, 1997).

4.5. Thermo-mechanical Analysis

Storage modulus curves that were derived from DMA data is illustrated in Figure 4.5.

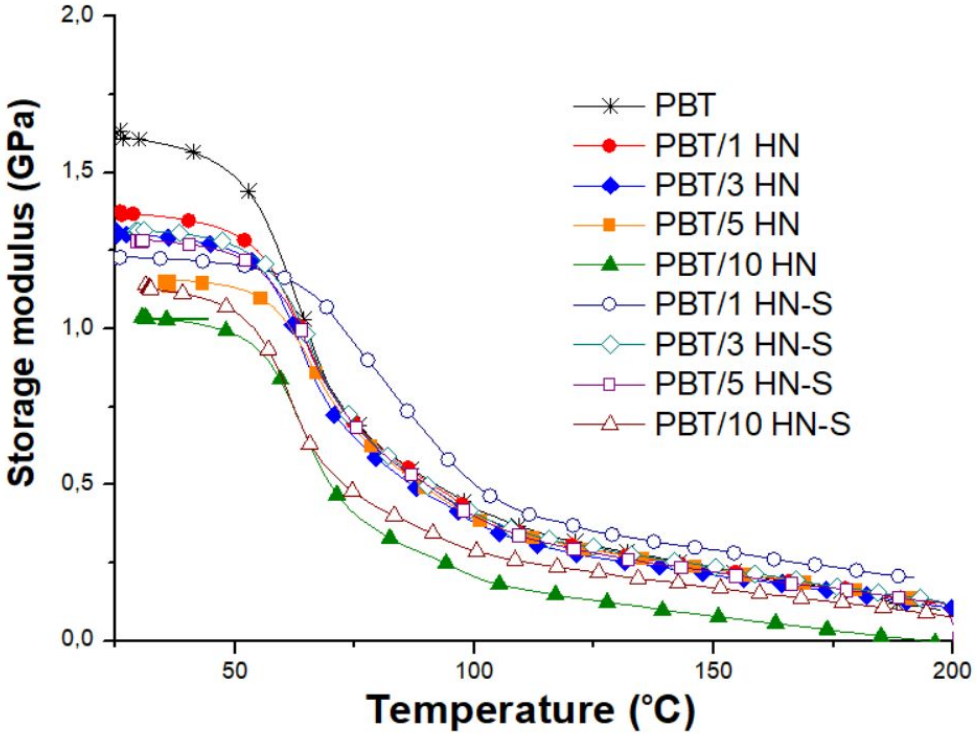

Figure 4.5 Storage modulus curves of PBT and composites

The dropping down of storage modulus curve of PBT in the temperature range of 50-100 ^{o}C is attributed to the relaxation of polymer chains due to the characteristic glass transition (Beaudoin et al., 1997; Ramakers-van Dorp et al., 2018). Initially, composites displayed lower storage modulus values with respect to PBT before this transition temperature. After that point, most of the composite samples reached the identical level of PBT in terms of storage modulus. As a different behavior, storage modulus values of composites involving HNT with the highest content (10%) were found to be lower than that of unfilled PBT. Silane modified HNT addition with the loading ratio of 1% gave higher storage modulus than PBT beyond the transition temperature. The highest storage modulus value was obtained for PBT/1 HN-S sample, as well.

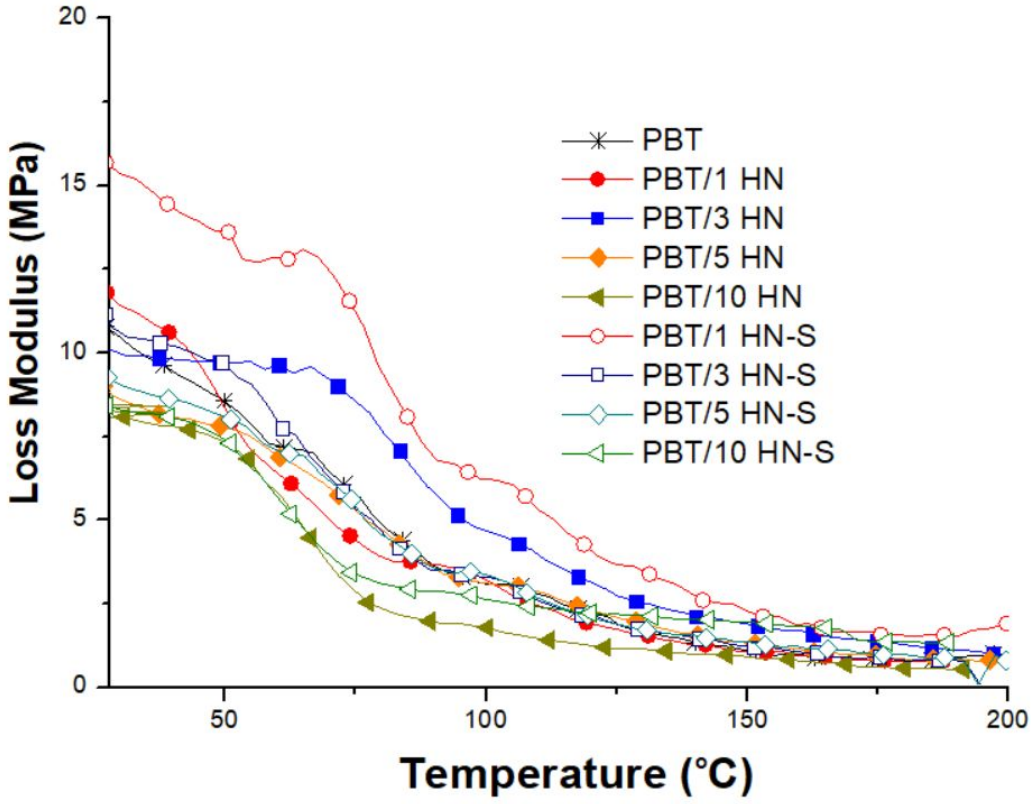

Figure 4.6 Loss modulus curves of PBT and composites

Loss modulus curves represented in Figure 4.6 implied that HNT inclusions with low filling amounts exhibited a positive influence on the loss modulus of PBT. Loss modulus values of composites reduced as HNT composition increased. As similar to storage modulus values, 1% content of HN-S compounded composite yielded a much higher loss modulus than other composites and the highest result was achieved for PBT/1 HN-S candidate.

Tan delta curves of PBT/HN and PBT/HN-S composites with respect to temperature are represented in Figure 4.7.

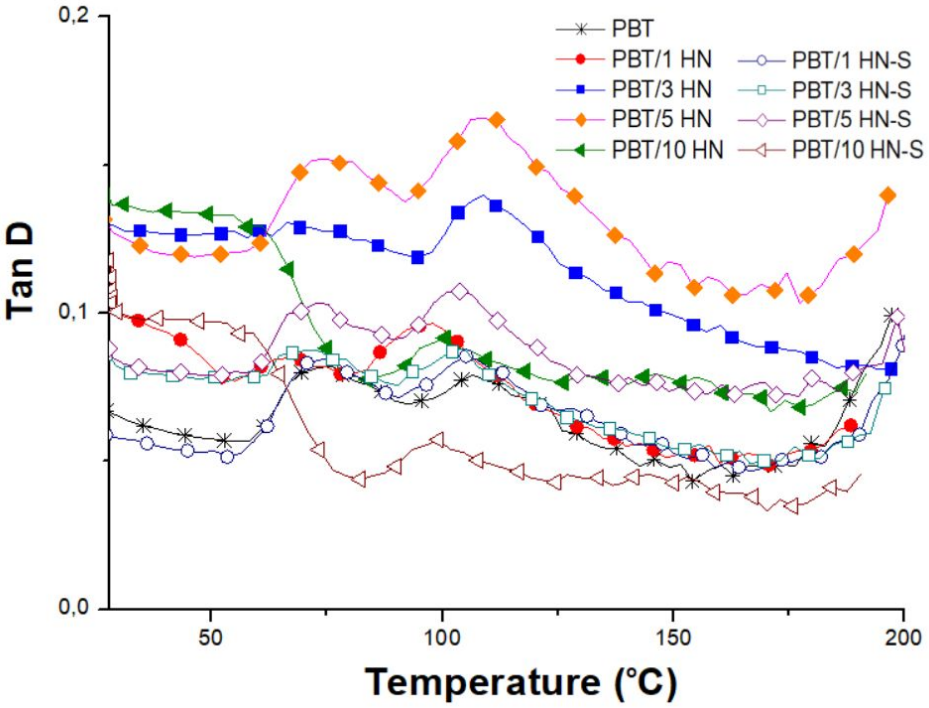

Figure 4.7 Tan delta curves of PBT and composites

According to Tan delta curves shown in Figure 4.7, the height of tan delta peak of composites filled with HN-S was found to be lower compared to unmodified HN-containing composites. Since the lowering in height of tan delta peak was linked to enhancement in interfacial adhesion of additive to polymer matrix in composite systems (Ashok et al., 2019; Bashir, 2021; Costa et al., 2016), silane-modified HNT loadings resulted in a reduction for Tan delta peak height. Similarly, 1% HN-S incorporated PBT yielded the best result thanks to the compatibilizer effect of the silane layer on the polymer-additive interface adhesion (Arslan and Dogan, 2018; Elkawash et al., 2020; Ramesh et al., 2022; Sismanoglu et al., 2021; Yang et al., 2019; Yildirimkaraman et al., 2020)

4.6. Thermal Gravimetric Analysis

The weight loss curves of PBT/HN and PBT/HN-S composites are in Figure 4.8 and Figure 4.9, respectively. Accordingly, thermal parameters of composites obtained by TGA analysis including temperature that 5% weight loss occurs ($T_{5\%}$), the temperature in which 10% weight loss occurs ($T_{10\%}$), a temperature that maxima on weight loss achieved ($T_{max\%}$), and the ratio of char residue over the total amount of samples are listed in Table 4.3.

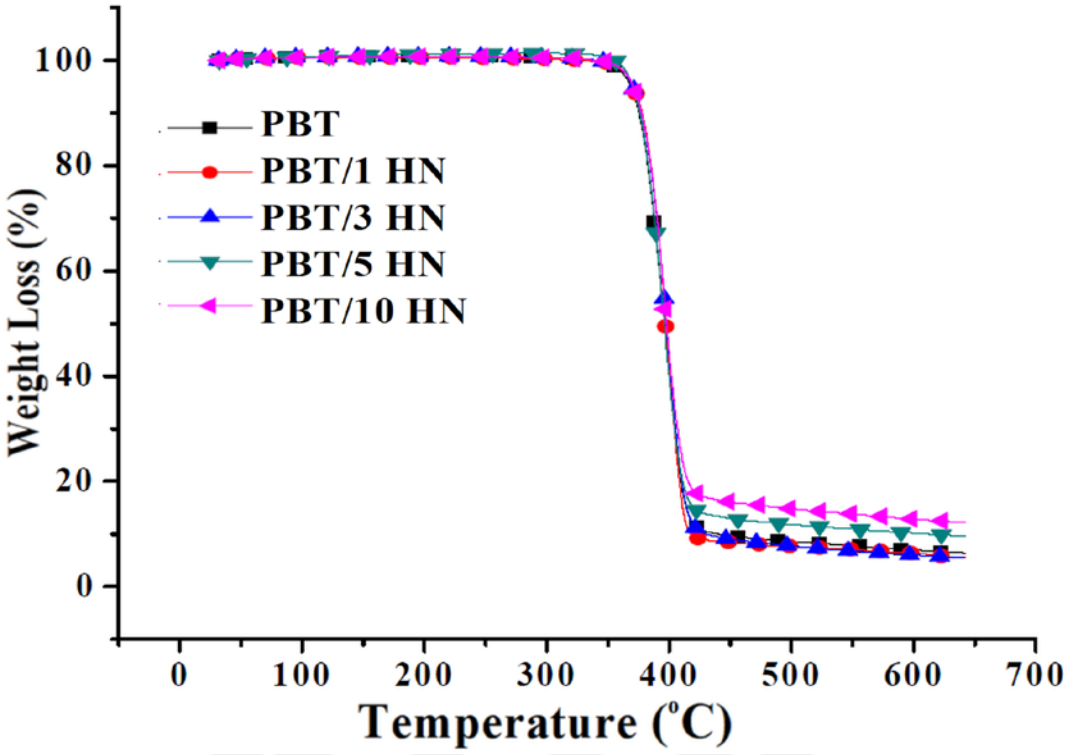

Figure 4.8 TGA curves of PBT/HN composites

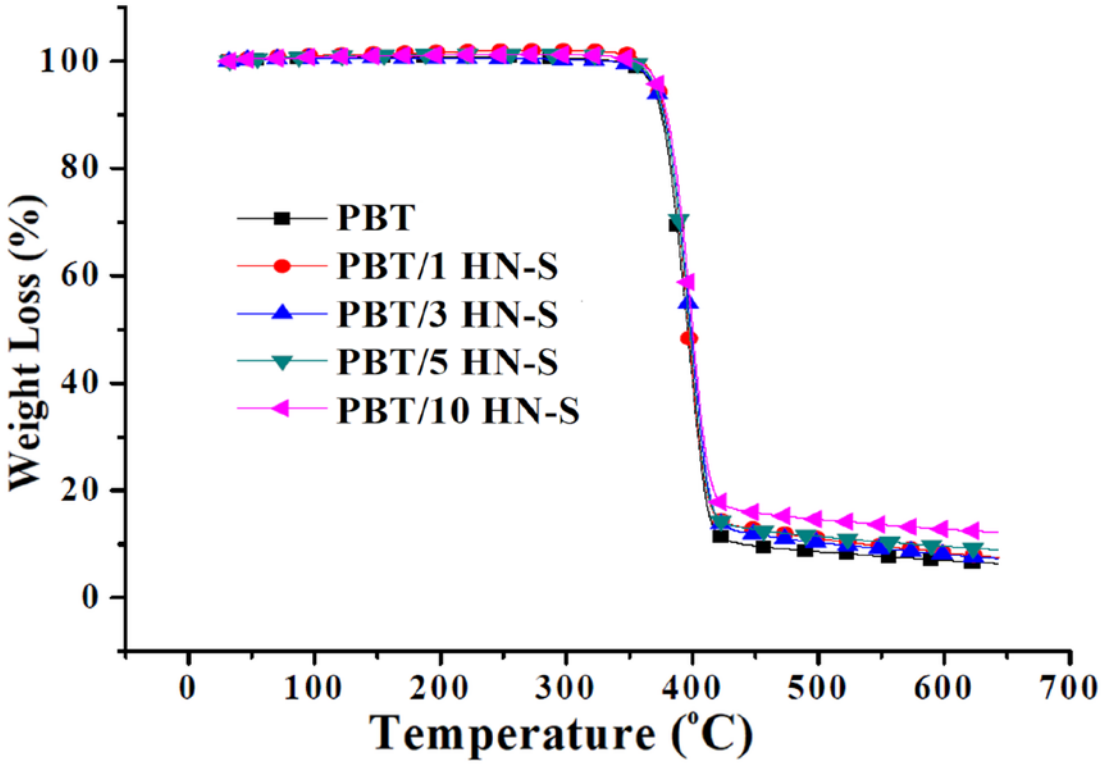

Figure 4.9 TGA curves of PBT/HN-S composites

Table 4.3 TGA data of PBT and relevant composites

Samples	$T_{5\%}$ (°C)	$T_{10\%}$ (°C)	T_{max} (°C)	residue (%)
PBT	365	373	398	5.8
PBT/ 1% HN	371	377	401	6.7
PBT/ 3% HN	370	377	400	8.1
PBT/ 5% HN	368	378	399	9.4
PBT/ 10% HN	359	375	398	13.6
PBT/ 1% HN-S	372	378	402	6.9
PBT/ 3% HN-S	370	377	401	7.7
PBT/ 5% HN-S	369	376	401	9.0
PBT/ 10% HN-S	357	373	399	12.5

The derivative weight loss curves of PBT/HN and PBT/HN-S composites are represented in Figure 4.10 and Figure 4.11, respectively.

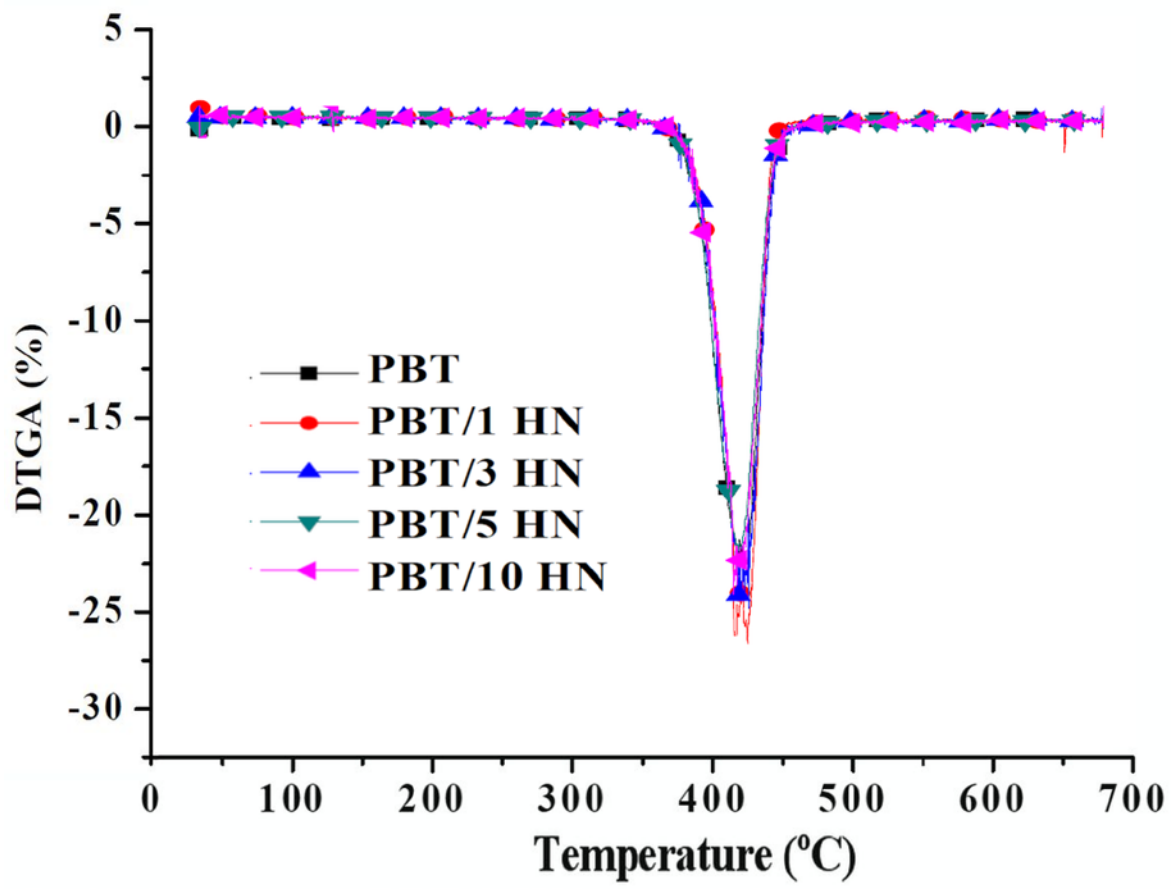

Figure 4.10 DTGA curves of PBT/HN composites

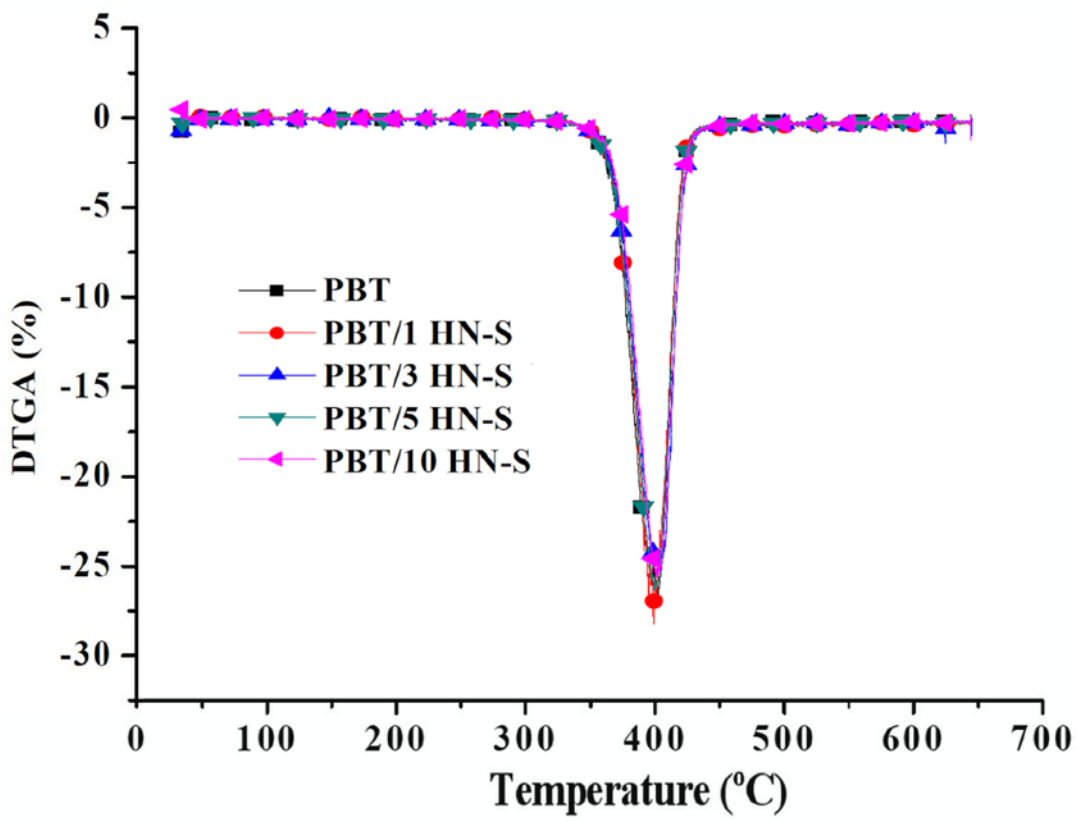

Figure 4.11 DTGA curves of PBT/HN-S composites

The weight loss of PBT occurs in a single step nearly 400 °C. An ionic breakdown mechanism results in the development of tetrahydrofuran during the first degradation period of PBT. This is followed by concerted ester pyrolysis reactions that produce 1,3-butadiene via an intermediate cyclic transition state. In both decomposition regimes, simultaneous decarboxylation reactions occur. Finally, the development of CO and complex aromatic compounds such as toluene, benzoic acid, and terephthalic acid was seen in the latter phases of decomposition of PBT structure (Botelho et al., 2001; Giannoni et al., 2003; Lum, 1979; Montaudo et al., 1993; Motori et al., 2000; Park et al., 2010; Passalacqua et al., 1976; Tan et al., 2010).

TGA thermographs in Figure 4.8 and Figure 4.9 revealed that thermal stability of PBT was not affected with HNT inclusions. However, the difference in thermal behaviors between PBT and composites was found to be more significant for DTGA curves relative to TGA curves. The peak temperature of DTGA curve indicates the maximum of mass loss rate is achieved (T_{max}) which corresponds to thermal decomposition of polymer.

According to TGA parameters in Table 4.3, initial decomposition temperatures ($T_{5\%}$ and $T_{10\%}$) of unfilled PBT increased with halloysite additions. Similarly, composites gave higher T_{max} values than T_{max} of PBT. The highest results were reached for 1% additive-containing composites as can be obtained from DTGA curves in Figure 4.10 and Figure 4.11. The shifting of these thermal parameters to higher temperatures corresponds to a reduction in the decomposition rate of polymer as well as improvement in thermal stability of polymers (Cirmad et al., 2022; Leszczynska and Pielichowski, 2008; Wunderlich, 2007). PBT/HN-S composites exhibited higher temperature parameters compared to composite samples involving unmodified HN. In other words, the silane layer on HN surface yielded enhancement in thermal resistance of PBT.

The decomposition of PBT was finalized at the end of the analysis by leaving a char with 5.8% residue content composed of organic compounds. The char yield value was found to be increased as the adding amount of HNT increased due to the thermally stable inorganic nature of HNT clay.

4.7. Melt Flow Rate Measurements

MFR values of PBT and relevant composites are indicated in bar chart format in Figure 4.12 and listed in Table 4.4.

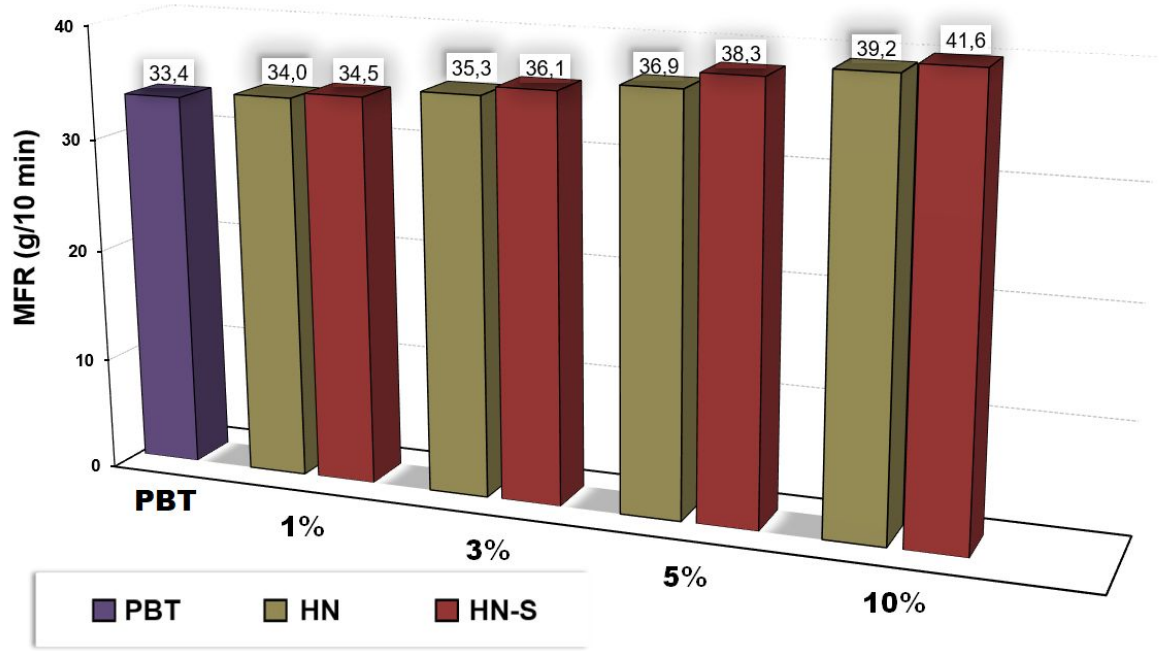

Figure 4.12 MFR test results of PBT and composites

The inclusion of HNT to PBT resulted in increments for MFR values regardless of HN grades. MFR of composites was extended as the amount of HNT increased. Similarly, Mohamed et al. (2020) reported that HNT additions caused improvement for MFR value of the polyurethane matrix (Mohamed et al., 2020). They postulated that the high aspect ratio of HNT clay was the main reason for that finding.

Relatively higher MFR parameters were achieved with silane-modified HN incorporated composites than MFR of PBT/HN composites at their identical loading levels. Improved interface adhesion of HNT clay to PBT matrix displayed a positive effect on melt-flow behavior of PBT.

4.8. Density Measurements

The measured densities of PBT and its composites are represented in Table 4.4.

Table 4.4 Density and MFR test results of PBT and composites

Additive/Content	**0 (PBT)**	**1%**	**3%**	**5%**	**10%**
HN	1.312±0.2	1.314±0.1	1.323±0.1	1.334±0.2	1.351±0.2
HN-S	1.312±0.2	1.318±0.1	1.330±0.2	1.337±0.1	1.356±0.2

The density of unfilled PBT increased slightly with 1% addition of HNT clay. The prominent improvements were observed for further inclusions of HN and HN-S. Silane modified HN grade exhibited higher density values than unmodified HN for their PBT-based composites.

4.9. SEM Studies

SEM micro-images of composites with x2,500, 5,000 and x10,000 magnifications are taken based on HNT compositions of 1%, 3%, 5%, and 10% and they were displayed accordingly as Figure 4.13, Figure 4.14, Figure 4.15, and Figure 4.16.

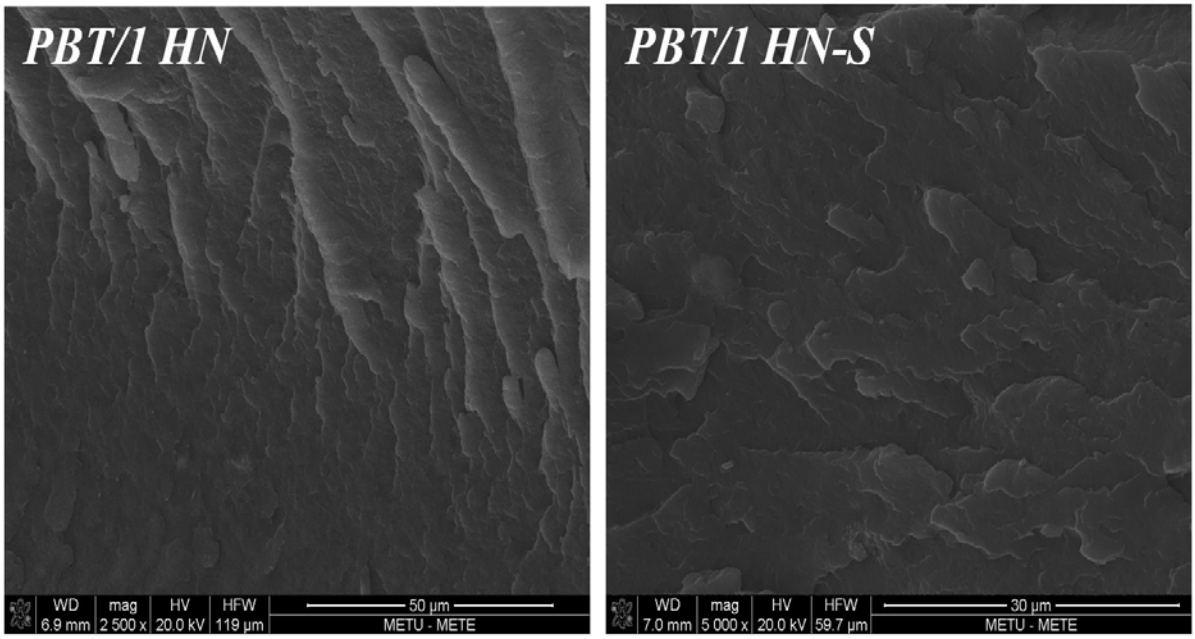

Figure 4.13 SEM micro-images of composites for 1% composition of HN and HN-S

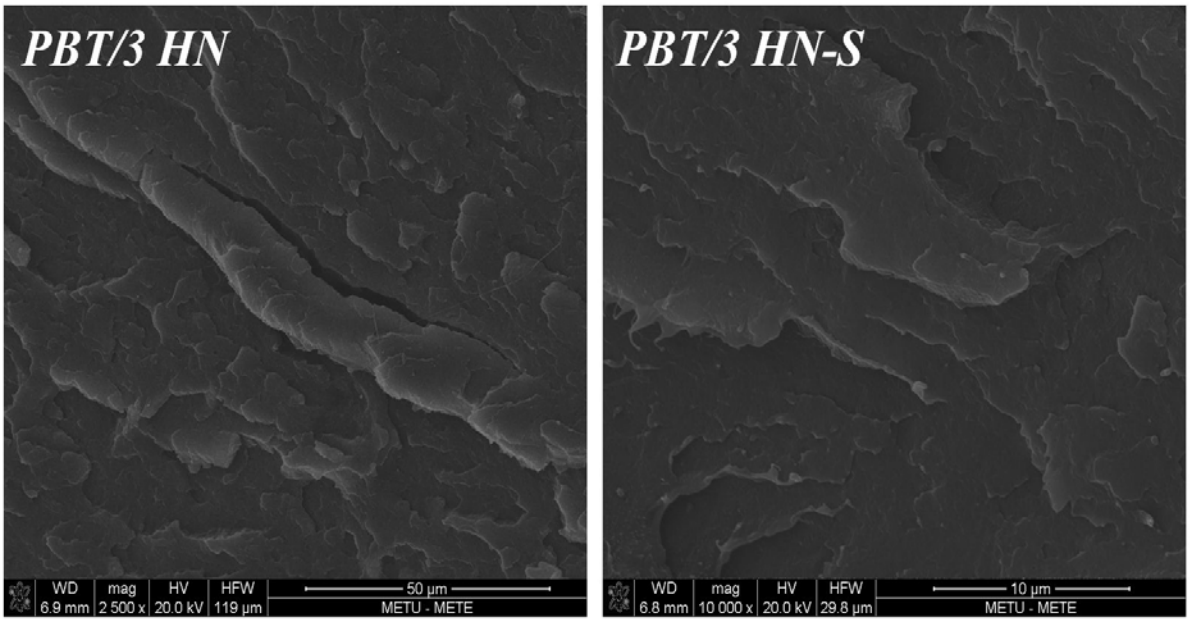

Figure 4.14 SEM micro-images of composites for 3% composition of HN and HN-S

According to SEM micro-images of composites involving 1% and 3% HNT, dispersions of HNT clays were found to be homogeneous. Silane modified layer of HN-S promoted dispersion uniformity of HNT particles into PBT phase stem from the enhanced interface interactions on PBT-HNT system.

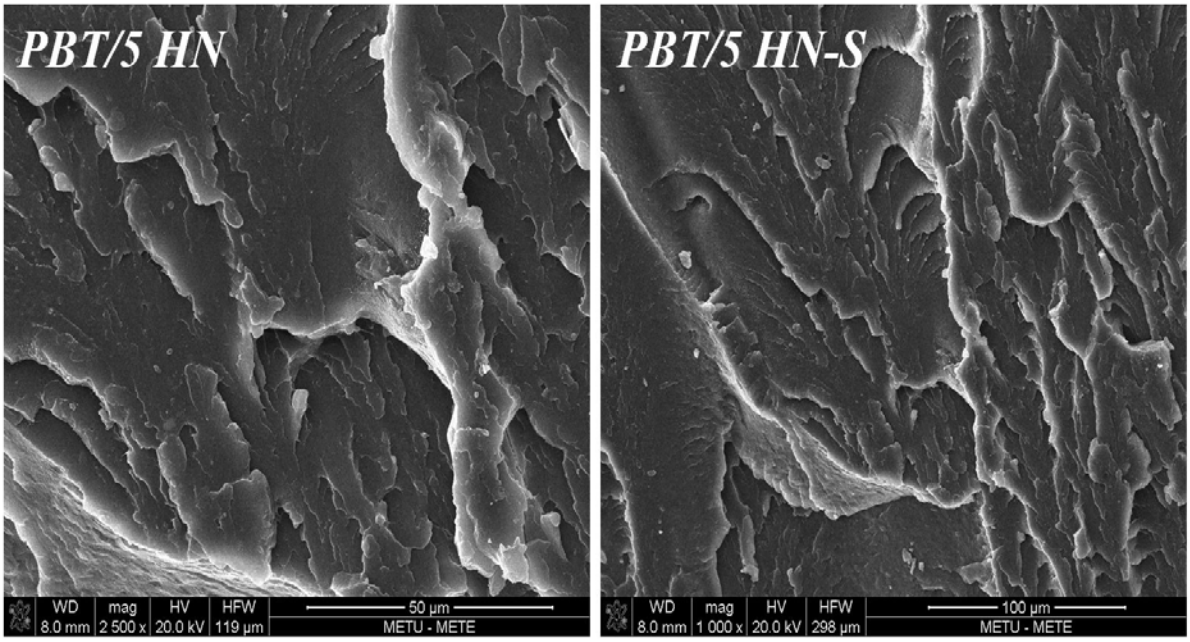

Figure 4.15 SEM micro-images of composites for 5% composition of HN and HN-S

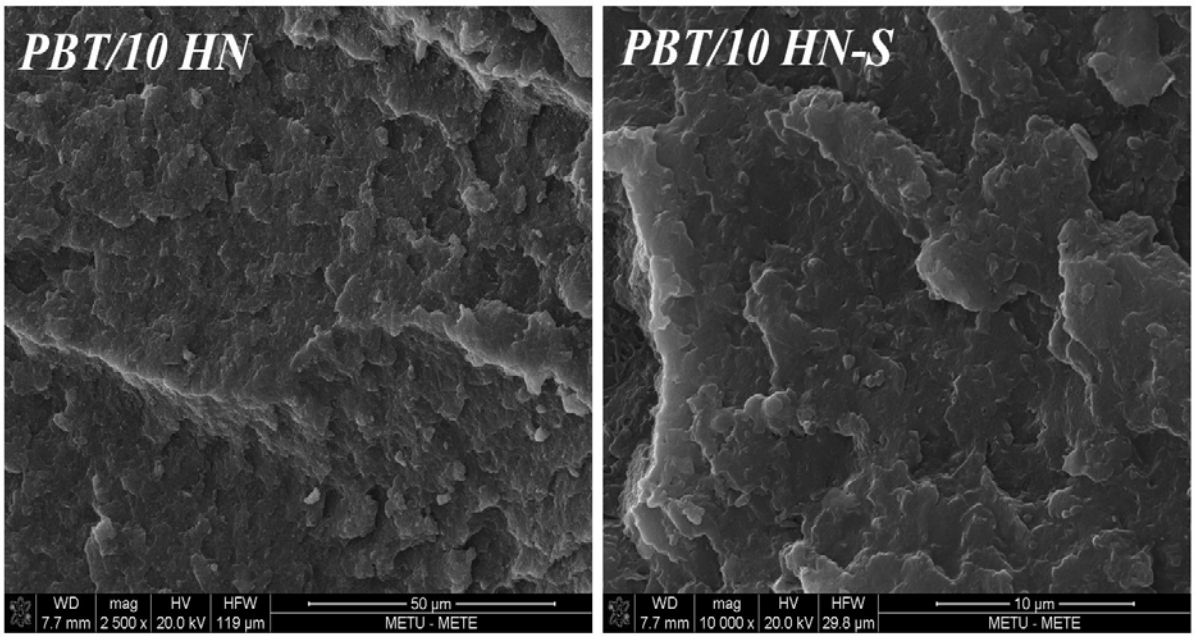

Figure 4.16 SEM micro-images of composites for 10% composition of HN and HN-S

SEM micro-images of composites containing highly-loaded HNT visualized that HNT particles started to stick together and form bundles into PBT matrix as their adding amounts increased. In contrast to composites involving the low amount of HNT, dispersion of clays was restricted as a result of the reduction in uniformity of mixing into PBT phase. The resulted bundle regions of HN were observed as highly indicative compared to HN-S.

5. CONCLUSIONS

In this thesis study, melt-blending method was applied to produce HNT-reinforced PBT composites. Two grades of commercial halloysite clay were used in the forms of pristine and silane-modified. Compounding of both HNT grades was taken place with four different contents using a lab-scale extruder. Test specimens of composites were shaped by an injection molding process.

During the characterization stage, tensile test, impact test, and hardness measurements were performed as mechanical characterization. Thermo-mechanical properties of composites were investigated with the help of DMA analysis. TGA test was conducted to characterize thermal behaviors. Density and MFR measurements were applied to evaluate physical properties and SEM technique was utilized to visualize the morphological characterization of halloysite containing PBT nanocomposites.

Tensile test results indicated that tensile strength, elongation, and tensile modulus values were improved with the low loading amounts of HNT inclusions. Silane modified grade displayed better performance compared to pristine HNT based on the tensile parameters.

Shore hardness of unfilled PBT was also enhanced after HNT additions regardless of their grades. An increasing trend of hardness values was obtained as the amount of HNT increased.

HNT additions led to an increase in impact strength of PBT. Similar to tensile properties, better impact performances were achieved for low concentrations of HNT. Silane modified HNT gave slightly higher impact strength with respect to unmodified HNT grade.

DMA study revealed that the lowest adding ratio of HNT displayed an increase in storage modulus as well as loss modulus. The relationship between the compatible silane layer of HNT surface and PBT matrix was confirmed by lowering the height of Tan delta curves of PBT/HN-S composite samples.

According to TGA test findings, HNT inclusions yielded a positive impact on the thermal resistance of PBT by causing a reduction in the decomposition rate of neat PBT. Composites filled with pristine HNT gave lower thermal performance compared to silane-modified HNT clay containing PBT.

A linear improvement in MFR parameter of PBT was obtained stem from the high aspect ratio of tubular HNT clay. Relatively higher MFR values were found for silane-modified HN than unmodified HN compounded composites.

The density of PBT exhibited no dramatic change by low amount loading of HNT. However, highly-filled composites showed a remarkable increase in density of PBT.

Property enhancements achieved for composite samples containing low contents of HNT were confirmed by SEM examinations in which uniform dispersion of HNT particles into PBT phase was observed. On the other hand, dispersion homogeneity of HNT reduced as its composition increased according to SEM images of highly-filled composite samples.

These conclusion remarks described that 1% adding amount was found to be the most suitable option in the case of investigated properties. Additionally, silane-modified grade displayed highly indicative improvements compared to pristine HNT clay due to better interfacial adhesion of HNT to PBT matrix was accomplished. As a result, PBT/ HN-S composite sample was bookmarked as the most suitable option to fabricate HNT reinforced PBT-based nanocomposites in terms of mechanical, thermo-mechanical, morphological, thermal, and physical performances according to findings in this study.

6. RECOMMENDATIONS

Based on the findings and conclusion remarks of this thesis study, the positive aspects of HNT additions to PBT-based nanocomposites were achieved in terms of examined behaviors. HNT-reinforced PBT composites can be extensively used in numerous applications owing to exclusive performances. Application fields of these developed composite materials cover a broad range since property improvements were reached on mechanical, thermal, and physical properties. The use of PBT in the cable and wire sector can be extended by HNT inclusions due to thermally stable PBT/HNT composites being reported. Additionally, PBT/HNT composite systems provide resistance to deformation in application fields where mechanically strong and durable materials are required. The transportation industry can be targeted industrial areas since the 1% HNT content inclusion resulted in a significant increase in mechanical strength, thermo-mechanical behavior and thermal resistance of PBT. Accordingly, low amount loading amounts of HNT gave negligible impact to density and melt-flow parameters which are related to weight saving and ease of processing of PBT-based composites, respectively. Development of composite parts used in automobile production would be considered because of the low-cost, low-weight, and mechanically strong characteristics of HNT-filled PBT composites. Silane modified halloysite grades exhibited better results and they were found to be more suitable in the case of discussed applications.

7. PUBLICATIONS

- Investigation of Strontium Master Alloy Addition Effect to Galfan (%95 Zn, %5 Al) Microstructure (DOI: 10.35414/akufemubid.826498)
- Investigation of corrosion properties strontium master alloy reinforced galfan (%95 Zn, %5 Al) alloy and applicability as coating on steel wire (Adana Alparslan Turkes Science and Technology University Journal of Science)

REFERENCES

Abdullah, Z. W., & Dong, Y. (2018). Preparation and characterisation of poly (vinyl) alcohol (PVA)/starch (ST)/halloysite nanotube (HNT) nanocomposite films as renewable materials. Journal of Materials Science, 53(5), 3455-3469.

Abdullah, Z. W., & Dong, Y. (2020). Polyvinyl Alcohol/Halloysite Nanotube Bionanocomposites as Biodegradable Packaging Materials. Springer, Singapore.

Akar, A. O., Yildiz, U. H., & Tayfun, U. (2021). Investigations of polyamide nano-composites containing bentonite and organo-modified clays: Mechanical, thermal, structural and processing performances. Reviews on Advanced Materials Science, 60(1), 293-302.

Akar, A. O., Yildiz, U. H., & Tayfun, U. (2022). Halloysite nanotube loaded polyamide nanocomposites: Structural, morphological, mechanical, thermal and processing behaviors. AIP Conference Proceedings, 432.

Allegra, G., Raos, G., & Vacatello, M. (2008). Theories and simulations of polymer-based nanocomposites: From chain statistics to reinforcement. Progress in Polymer Science, 33(7), 683-731.

Altan, T. A., Lilly, B. W., Kruth, J. P., König, W., Tönshoff, H. K., Van Luttervelt, C. A., & Khairy, A. B. (1993). Advanced techniques for die and mold manufacturing. CIRP annals, 42(2), 707-716.

Arat, R., & Uyanık, N. (2017). Surface modification of nanoclays with styrene-maleic anhydride copolymers. Natural Resources, 8(03), 159.

Arslan, C., & Dogan, M. (2018). The effects of silane coupling agents on the mechanical properties of basalt fiber reinforced poly(butylene terephthalate) composites. Composites Part B, 146, 145–154.

Ashok, R. B., Srinivasa, C. V., & Basavaraju, B. (2019). Dynamic mechanical properties of natural fiber composites—a review. Advanced Composites and Hybrid Materials, 2(4), 586-607.

Athimoolam, M., & Moorthy, T. V. (2012). Polymer Nanocomposite Materials and shape memory applications-A Review. Procedia Engineering, 38, 3399-3408.

Bährle-Rapp M. (2007) Polybutylene Terephthalate. In: Springer Lexikon Kosmetik und Körperpflege. Springer, Berlin

Bashir, M. A. (2021). Use of dynamic mechanical analysis (DMA) for characterizing interfacial interactions in filled polymers. Solids, 2(1), 108-120.

Baxi, R. N., Pathak, S. U., & Peshwe, D. R. (2011). Impact modification of a PET–PBT blend using different impact modifiers. Polymer Journal, 43(9), 801-808.

Beake, B.D., Goodes, S.R., Smith, J.F. & Gao, F. (2004). Nanoscale repetitive impact testing of polymer films. Journal of Materials Research, 19(1), 237-247.

Beaudoin, O., Bergeret, A., Quantin, J. C., & Crespy, A. (1997). Viscoelastic behaviour of glass beads reinforced poly (butylene terephthalate): experimental and theoretical approaches. Composite Interfaces, 5(6), 543-559.

Belofsky, H. (1995). Plastics: Product Design and Process Engineering. Munich: Hanser, Carl Verlag.

Bharatiya, D., Patra, S., Parhi, B., & Swain, S. K. (2021). A materials science approach towards bioinspired polymeric nanocomposites: a comprehensive review. International Journal of Polymeric Materials and Polymeric Biomaterials, 1-16.

Bogue, R. (2011). Nanocomposites: a review of technology and applications. Assembly Automation, 31(2), 106-112.

Botelho, G., Queirós, A., Liberal, S., & Gijsman, P. (2001). Studies on thermal and thermo-oxidative degradation of poly (ethylene terephthalate) and poly (butylene terephthalate). Polymer Degradation and Stability, 74(1), 39-48.

Brantseva, T. V., Antonov, S. V., & Gorbunova, I. Y. (2018). Adhesion properties of the nanocomposites filled with aluminosilicates and factors affecting them: a review. International Journal of Adhesion and Adhesives, 82, 263-281.

Bratovčić, A., Odobašić, A., Ćatić, S., & Šestan, I. (2015). Application of polymer nanocomposite materials in food packaging. Croatian Journal of Food Science and Technology, 7(2), 86-94.

Camargo, P. H. C., Satyanarayana, K. G., & Wypych, F. (2009). Nanocomposites: synthesis, structure, properties and new application opportunities. Materials Research, 12(1), 1-39.

Chabot Jr, J. F., & Malloy, R. (1997). History of thermoplastic injection molding. Part I: The birth of an industry. Journal of Injection Molding Technology, 1(1), 1-9.

Chaiwutthinan, P., Riyaphan, T., Simpraditpan, A., Larpkasemsuk, A. (2020). Influence of poly (butylene terephthalate) and wollastonite on properties of recycled poly (ethylene terephthalate) preforms. Journal of Metals, Materials and Minerals, 30(1), 173.

Cheng, C., Song, W., Zhao, Q., & Zhang, H. (2020). Halloysite nanotubes in polymer science: Purification, characterization, modification and applications. Nanotechnology Reviews, 9(1), 323-344.

Cheng, Z. L., Chang, X. Y., Liu, Z., Qin, D. Z. (2018). Surface-modified halloysite nanotubes as fillers applied in reinforcing the performance of polytetrafluoroethylene. Clay Minerals, 53, 643–656

Cheremisinoff, N. P. (1987). Polymer Mixing and Extrusion Technology. CRC Press, Boca Raton.

Chval, Z., Raz, K., & Sedlacek, F. (2020). Design of injection mold from plastic material. Key Engineering Materials, 847, 75-80.

Cirmad, H., Tirkes, S., & Tayfun, U. (2022). Evaluation of flammability, thermal stability and mechanical behavior of expandable graphite-reinforced acrylonitrile–butadiene–styrene terpolymer. Journal of Thermal Analysis and Calorimetry, 147, 2229–2237.

Correia Diogo, A. (2015). Polymers in building and construction. In Materials for Construction and Civil Engineering (pp. 447-499). Springer, Switzerland.

Costa, C. S. M. F., Fonseca, A. C., Serra, A. C., & Coelho, J. F. J. (2016). Dynamic mechanical thermal analysis of polymer composites reinforced with natural fibers. Polymer Reviews, 56(2), 362-383.

Cunha, S. M., Gaspar, A., & Covas, J. A. (2009). Melting of polymer blends in single-screw extrusion-an experimental study. International Journal of Material Forming, 2(1), 729-732.

Deshmukh, G. S., Peshwe, D. A., Pathak, S. U., & Ekhe, J. D. (2011). A study on effect of mineral additions on the mechanical, thermal, and structural properties of poly (butylene terephthalate) (PBT) composites. Journal of Polymer Research, 18(5), 1081-1090.

Doagou-Rad, S., Islam, A., & Merca, T. D. (2020). An application-oriented roadmap to select polymeric nanocomposites for advanced applications: A review. Polymer Composites, 41(4), 1153-1189.

Dogossy, G., Sági, E., & Ronkay, F. (2013). Investigation of Mixing Processes of Polymer Composites. Materials Science Forum, 729, 332-337.

Duce, C., Vecchio Ciprioti, S., Ghezzi, L., Ierardi, V., & Tine, M. R. (2015). Thermal behavior study of pristine and modified halloysite nanotubes. Journal of Thermal Analysis and Calorimetry, 121(3), 1011-1019.

Ebrahimi, F., & Dabbagh, A. (2019). A comprehensive review on modeling of nanocomposite materials and structures. Journal of Computational Applied Mechanics, 50(1), 197-209.

Elkawash, H., Tirkes, S., Hacioglu, F., & Tayfun, U. (2020). Physical and mechanical performance of bentonite and barite loaded low density polyethylene composites: Influence of surface silanization of minerals. Journal of Composite Materials, 54(28), 4359-4368.

Erpek, C. E. Y., Ozkoc, G., & Yilmazer, U. (2016). Effects of halloysite nanotubes on the performance of plasticized poly (lactic acid)-based composites. Polymer Composites, 11(37), 3134-3148.

Erpek, C. E. Y., Ozkoc, G., & Yilmazer, U. (2017). Comparison of natural halloysite with synthetic carbon nanotubes in poly (lactic acid) based composites. Polymer Composites, 38(11), 2337-2346.

Ertas, M., Altuntas, E., & Donmez Cavdar, A. (2019). Effects of halloysite nanotube on the performance of natural fiber filled poly (lactic acid) composites. Polymer Composites, 40(11), 4238-4247.

Ezenkwa, O. E., Hassan, A., Samsudin, S. A. (2022). Comparison of mechanical properties and thermal stability of graphene-based materials and halloysite nanotubes reinforced maleated polymer compatibilized polypropylene nanocomposites. Polymer Composites, DOI: 10.1002/pc.26503

Farhoodi, M. (2016). Nanocomposite materials for food packaging applications: characterization and safety evaluation. Food Engineering Reviews, 8(1), 35-51.

Fu, H., Xu, H., Liu, Y., Yang, Z., Kormakov, S., Wu, D., & Sun, J. (2020). Overview of injection molding technology for processing polymers and their composites. ES Materials & Manufacturing, 8, 3-23.

Fu, S., Sun, Z., Huang, P., Li, Y., & Hu, N. (2019). Some basic aspects of polymer nanocomposites: A critical review. Nano Materials Science, 1(1), 2-30.

Garcia-Escobar, F., Bonilla-Rios, J., Espinoza-Martinez, A. B., & Cerda-Hurtado, P. (2021). Halloysite silanization in polyethylene terephthalate composites for bottling and packaging applications. Journal of Materials Science, 56(29), 16376-16386.

Gerasin, V.A., Antipov, E.M., Karbushev, V.V., Kulichikhin, V.G., Karpacheva, G.P., Talroze, R.V., & Kudryavtsev, Y.V. (2013). New approaches to the development of hybrid nanocomposites: from structural materials to hightech applications. Russian Chemical Reviews, 82, 303.

Giannoni, S., Montanari, G.C., Motori, A. and Saccani, A. (2003). Thermal endurance evaluation of poly (butylene terephthalate) by conventional and analytical methods. Journal of materials research, 18(6), pp.1342-1346.

Giles H.F., Wagner J.R., Mount E.M. (2005). Extrusion The Definitive Processing Guide and Handbook. William Andrew Publishing, New York.

Goda, E. S., Yoon, K. R., El-sayed, S. H., & Hong, S. E. (2018). Halloysite nanotubes as smart flame retardant and economic reinforcing materials: A review. Thermochimica acta, 669, 173-184.

Guo, B., Zou, Q., Lei, Y., & Jia, D. (2009). Structure and performance of polyamide 6/halloysite nanotubes nanocomposites. Polymer, 41(10), 835-842.

Hage, E., Hale, W., Keskkula, H., & Paul, D. R. (1997). Impact modification of poly (butylene terephthalate) by ABS materials. Polymer, 38(13), 3237-3250.

Harito, C., Bavykin, D. V., Yuliarto, B., Dipojono, H. K., & Walsh, F. C. (2019). Polymer nanocomposites having a high filler content: synthesis, structures, properties, and applications. Nanoscale, 11(11), 4653-4682.

Hillier, S., Brydson, R., Delbos, E., Fraser, T., Gray, N., Pendlowski, H., Phillips, I., Robertson, J., & Wilson, I. (2016). Correlations among the mineralogical and physical properties of halloysite nanotubes (HNTs). Clay Minerals, 51, 325–350.

Hope, E. W., Kittrick, J. A. (1964). Surface tension and the morphology of halloysite. American Mineralogist: Journal of Earth and Planetary Materials, 49, 859–866.

Huang, J., Tang, Z.H., Zhang, X.H., & Guo, B.C. (2016). Halloysite Polymer Nanocomposites. In: Nanosized Tubular Clay Minerals. Developments in Clay Science, Elsevier, Amsterdam.

Hussain, F., Hojjati, M., Okamoto, M., & Gorga, R. E. (2006). Polymer-matrix nanocomposites, processing, manufacturing, and application: an overview. Journal of Composite Materials, 40(17), 1511-1575.

Hyvärinen, M., Jabeen, R., & Kärki, T. (2020). The modelling of extrusion processes for polymers-A review. Polymers, 12(6), 1306.

Idumah, C. I., Hassan, A., Ogbu, J., Ndem, J. U., & Nwuzor, I. C. (2019). Recently emerging advancements in halloysite nanotubes polymer nanocomposites. Composite Interfaces, 26(9), 751-824.

Isayev, A. I. (2000). Molding processes. In Handbook of Industrial Automation (pp. 573-606). CRC Press.

Ito, E. N., Ueki, M. M., Bretas, R. E. S., & Hage Junior, E. (2008). Interfacial tension of PBT/SAN blends by the drop retraction method. Materials Research, 11(2), 165-169.

Jancar, J., Douglas, J. F., Starr, F. W., Kumar, S. K., Cassagnau, P., Lesser, A. J., Sternstein, S. S. & Buehler, M. J. (2010). Current issues in research on structure–property relationships in polymer nanocomposites. Polymer, 51(15), 3321-3343.

Jasinski, E., Bounor-Legaré, V., Taguet, A., & Beyou, E. (2021). Influence of halloysite nanotubes onto the fire properties of polymer based composites: A review. Polymer Degradation and Stability, 183, 109407.

Jia, Z., Luo, Y., Guo, B., Yang, B., Du, M., & Jia, D. (2009). Reinforcing and flame-retardant effects of halloysite nanotubes on LLDPE. Polymer-Plastics Technology and Engineering, 48(6), 607-613.

Jing, H., Higaki, Y., Ma, W., Wu, H., Yah, W. O., Otsuka, H., Lvov, Y. M., & Takahara, A. (2013). nternally modified halloysite nanotubes as inorganic nanocontainers for a flame retardant. Chemistry letters, 42(2), 121-123.

Joussein, E., Petit, S., Churchman, J., Theng, B., Righi, D., & Delvaux, B. (2005). Halloysite clay minerals–a review. Clay Minerals, 40, 383–426.

Kausar, A. (2018). Review on polymer/halloysite nanotube nanocomposite. Polymer-Plastics Technology and Engineering, 57(6), 548-564.

Kent, R. (2006). Cost Management in Plastics Processing Strategies, Targets, Techniques and Tools. Rapra Technology Limited, London.

Khunová, V., Kelnar, I., Kristóf, J., Dybal, J., Kratochvíl, J., & Kaprálková, L. (2015). The effect of urea and urea-modified halloysite on performance of PCL. Journal of Thermal Analysis and Calorimetry, 120(2), 1283-1291.

Khunova, V., Kristóf, J., Kelnar, I., & Dybal, J. (2013). The effect of halloysite modification combined with in situ matrix modifications on the structure and properties of polypropylene/halloysite nanocomposites. eXPRESS Polymer Letters, 7(5).

Kim, Y. H., Park, S. J., & Nakagaito, A. N. (2017). Optimization of processing condition of manocomposites according to the structural changes of halloysite nanotubes under impact behavior. Metallurgical and Materials Transactions B, 48(4), 1933-1937.

Kohlgrüber, K. (Ed.). (2012). Co-rotating Twin-screw Extruder. Munich: Carl Hanser Verlag.

Kong, W., Wang, W., Gao, J., Liu, T., & Liu, Y. (2011). Oxidized starch films reinforced with natural halloysite. Journal of Materials Research, 26(23), 2938-2944.

Lafleur, P. G., & Vergnes, B. (2014). Polymer Extrusion. Wiley, New Jersey.

Leszczynska, A., & Pielichowski, K. (2008). Application of thermal analysis methods for characterization of polymer/montmorillonite nanocomposites. Journal of thermal analysis and calorimetry, 93(3), 677-687.

Lewandowski, A., & Wilczyński, K. (2022). Modeling of twin screw extrusion of polymeric materials. Polymers, 14(2), 274.

Liu, M., Guo, B., Zou, Q., Du, M., & Jia, D. (2008). Interactions between halloysite nanotubes and 2, 5-bis (2-benzoxazolyl) thiophene and their effects on reinforcement of polypropylene/halloysite nanocomposites. Nanotechnology, 19(20), 205709.

Liu, M., Jia, Z., Jia, D., & Zhou, C. (2014). Recent advance in research on halloysite nanotubes-polymer nanocomposite. Progress in polymer science, 39(8), 1498-1525.

Liu, M., Zhang, Y., & Zhou, C. (2013). Nanocomposites of halloysite and polylactide. Applied Clay Science, 75, 52-59.

Lum, R. M. (1979). Thermal decomposition of poly (butylene terephthalate). Journal of Polymer Science: Polymer Chemistry Edition, 17(1), 203-213.

Lun, H., Ouyang, J., & Yang, H. (2014). Enhancing dispersion of halloysite nanotubes via chemical modification. Physics and Chemistry of Minerals, 41(4), 281-288.

Manocha, L. M., Valand, J., Patel N, Warrier, A., & Manocha, S. (2006). Nanocomposites for structural applications. Journal of Pure and Applied Physics, 44, 135–142.

Manuel, H. J., & Gaymans, R. J. (1993). Segmented block copolymers based on dimerized fatty acids and poly (butylene terephthalate). Polymer, 34(3), 636-641.

Massaro, M., Lazzara, G., Noto, R., & Riela, S. (2020). Halloysite nanotubes: A green resource for materials and life sciences. Rendiconti Lincei. Scienze Fisiche e Naturali, 31(2), 213-221.

McNally, D., Gall, J. S. (1986) The History of Poly(Butylene Terephthalate) Molding Resins. In: Seymour R.B., Kirshenbaum G.S. (eds) High Performance Polymers: Their Origin and Development. Springer, Dordrecht.

Mittal, V. (2009). Optimization of Polymer Nanocomposite properties. Wiley, New York.

Mohamed, S. T., Tirkes, S., Akar, A. O., & Tayfun, U. (2020). Hybrid nanocomposites of elastomeric polyurethane containing halloysite nanotubes and POSS nanoparticles: tensile, hardness, damping and abrasion performance. Clay Minerals, 55(4), 281-292.

Montaudo, G., Puglisi, C., & Samperi, F. (1993). Primary thermal degradation mechanisms of PET and PBT. Polymer degradation and stability, 42(1), 13-28.

Motori, A., Montanari, G.C., Saccani, A. & Giannoni, S. (2000). Effect of recrystallization on the oxidative stability of poly (butylene terephthalate). Journal of Materials Research, 15(1), 243-247.

Moazeni, N., Mohamad, Z. & Dehbari, N. (2015). Study of silane treatment on poly-lactic acid(PLA)/Sepiolite nanocomposite thin films. Journal of Applied Polymer Science, 132, 41428.

Nazir, M. S., Mohamad Kassim, M. H., Mohapatra, L., Gilani, M. A., Raza, M. R., & Majeed, K. (2016). Characteristic properties of nanoclays and characterization of nanoparticulates and nanocomposites. In Nanoclay reinforced polymer composites (pp. 35-55). Springer, Singapore.

Oburoğlu, N., Ercan, N., Durmus, A., Kaşgöz, A. (2012). Effects of halloysite nanotube on the mechanical properties and nonisothermal crystallization kinetics of poly (butylene terephthalate) (PBT). Journal of Macromolecular Science Part B, 51(5), 860-879.

Owoseni, O., Zhang, Y., Su, Y., He, J., McPherson, G. L., Bose, A., John, V. T. (2015). Tuning the wettability of halloysite clay nanotubes by surface carbonization for optimal emulsion stabilization. Langmuir, 31, 13700–13707.

Pal, P., Kundu, M. K., Malas, A., & Das, C. K. (2014). Compatibilizing effect of halloysite nanotubes in polar–nonpolar hybrid system. Journal of Applied Polymer Science, 131(1), 39587.

Park, J. M., Lee, J. Y., & Park, Y. H. (2010). Eco-friendly flame retardant poly (butylene terephthalate) copolymers with thermal stability and hydrolytic resistance. Macromolecular Research, 18(6), 539-544.

Passalacqua, V., Pilati, F., Zamboni, V., Fortunato, B., & Manaresi, P. (1976). Thermal degradation of poly (butylene terephthalate). Polymer, 17(12), 1044-1048.

Patil, A., Patel, A., & Purohit, R. (2017). An overview of polymeric materials for automotive applications. Materials Today: Proceedings, 4(2), 3807-3815.

Paul, D. R., & Robeson, L. M. (2008). Polymer nanotechnology: nanocomposites. Polymer, 49(15), 3187-3204.

Prashantha, K., Lecouvet, B., Sclavons, M., Lacrampe, M. F., & Krawczak, P. (2013). Poly (lactic acid)/halloysite nanotubes nanocomposites: Structure, thermal, and mechanical properties as a function of halloysite treatment. Journal of Applied Polymer Science, 128(3), 1895-1903.

Ram, A. (1997). Description of major plastics: Structure, properties and utilization. In Fundamentals of Polymer Engineering (pp. 148-215). Springer, Boston.

Ramakers-van Dorp, E., Haenel, T., Sturm, F., Möginger, B., & Hausnerova, B. (2018). On merging DMA and microindentation to determine local mechanical properties of polymers. Polymer Testing, 68, 359-364.

Ramesh, M., Rajeshkumar, L., Balaji, D., & Bhuvaneswari, (2022). Influence of Moisture Absorption on Mechanical properties of Biocomposites reinforced Surface Modified Natural Fibers. Aging Effects on Natural Fiber-Reinforced Polymer Composites: Durability and Life Prediction, Springer, Singapore.

Rawtani, D., Agrawal, Y.K. (2012). Multifarious applications of halloysite nanotubes: A review. Reviews on Advanced Materials Science, 30, 282-295.

Rosato, D. V., & Rosato, M. G. (2012). Injection Molding Handbook. Springer, Berlin.

Rubin, I. I. (1990). Handbook of Plastic Materials and Technology. Wiley, New York.

Sagare, R. D., Dasankoppa, F. S., Sholapur, H. N., & Burga, K. (2021). Halloysite nanotubes: Design, characterization and applications. A review. Farmacia, 69, 208-214.

Saurabh, K., Park, H. S. and Lee, C. M. (2020). Data-driven smart control of injection molding process. CIRP Journal of Manufacturing Science and Technology, 31, 439-449.

Scheirs, J., & Long, T. E. (2005). Modern Polyesters: Chemistry and Technology of Polyesters and Copolyesters. Wiley, New York.

Silvestre, J., Silvestre, N., & De Brito, J. (2016). Polymer nanocomposites for structural applications: Recent trends and new perspectives. Mechanics of Advanced Materials and Structures, 23, 1263–1277.

Sismanoglu, S., Tayfun, U., Popescu, C. M., & Kanbur, Y. (2021). Effective use of olive pulp as biomass additive for eco-grade TPU-based composites using functional surface modifiers. Biomass Conversion and Biorefinery, 1-16.

Speranza, V., Vietri, U. and Pantani, R. (2011). Monitoring of injection molding of thermoplastics: Average solidification pressure as a key parameter for quality control. Macromolecular Research, 19(6), 542.

Tan, L., Chen, Y., Wang, Y., Zhou, W., & He, X. (2010). Melt reaction and structural analysis based on poly (butylene terephthalate) and oligo (lactic acid) with addition of butanediol. Journal of thermal analysis and calorimetry, 99(1), 269-275.

Tham, W. L., Poh, B. T., Mohd Ishak, Z. A., & Chow, W. S. (2016). Transparent poly (lactic acid)/halloysite nanotube nanocomposites with improved oxygen barrier and antioxidant properties. Journal of Thermal Analysis and Calorimetry, 126(3), 1331-1337.

Utracki L.A. (2004). Clay Containing Polymeric Nanocomposites. 1st Edition, Rapra, London.

Van Berkel, R. W. M., Van Hartingsveldt, E. A., & Van der Sluijs, C. L. (1997). Polybutylene Terephthalate. In: Handbook of Thermoplastics, Marcel Deccer, New York.

Velmurugan, R., & Mohan, T. P. (2004). Room temperature processing of epoxy-clay nanocomposites. Journal of Materials Science, 39(24), 7333-7339.

Vergnes, B., Souveton, G., Delacour, M. L., & Ainser, A. (2001). Experimental and theoretical study of polymer melting in a co-rotating twin screw extruder. International Polymer Processing, 16(4), 351-362.

Vilela, C., Sousa, A. F., Fonseca, A. C., Serra, A. C., Coelho, J. F., Freire, C. S., & Silvestre, A. J. (2014). The quest for sustainable polyesters–insights into the future. Polymer Chemistry, 5(9), 3119-3141.

Vinyas, M., Athul, S. J., Harursampath, D., Loja, M., & Thoi, T. N. (2019). A comprehensive review on analysis of nanocomposites: from manufacturing to properties characterization. Materials Research Express, 6(9), 092002.

Viswanathan, V., Laha, T., Balani, K., Agarwal, A., & Seal, S. (2006). Challenges and advances in nanocomposite processing techniques. Materials Science and Engineering: R: Reports, 54(5-6), 121-285.

Wilczynski, K., & White, J. L. (2003). Melting model for intermeshing counter-rotating twin-screw extruders. Polymer Engineering & Science, 43(10), 1715-1726.

Wood, S. L., & Ullman, D. G. (1996). The functions of plastic injection moulding features. Design Studies, 17(2), 201-213.

Wu, W., Zhao, W., Gong, X., Sun, Q., Cao, X., Su, Y., & Vellaisamy, R. A. (2022). Surface decoration of halloysite nanotubes with POSS for fire-safe thermoplastic polyurethane nanocomposites. Journal of Materials Science & Technology, 101, 107-117.

Wunderlich, B. (2007). Thermal analysis of macromolecules: a personal review. Journal of thermal analysis and calorimetry, 89(2), 321-356.

Yang, K., Chi, Q., Wang, X., Jiang, Y., Li, F., & Xue, B. (2019). The role of halloy site on crystallinity, ion conductivity, thermal and mechanical properties of poly (ethylene-oxide)/halloysite nanocomposites. Journal of Polymer Research, 26(6), 1-11.

Yen, C. W. (1996). Plastic Molding Design and Mechanical Design. OpenTech, Taipei.

Yildirimkaraman, O., Yildiz, U. H., Akar, A. O., & Tayfun, U. (2020). Evaluation of water repellency in bentonite filled polypropylene composites via physical and mechanical methods. IOP SciNotes, 1(2), 024804.

Yuan, P., Tan, D., & Annabi-Bergaya, F. (2015). Properties and applications of halloysite nanotubes: recent research advances and future prospects. Applied Clay Science, 112, 75-93.

Zeng, Q. H., Yu, A. B., Lu, G. Q., & Paul, D. R. (2005). Clay-based polymer nanocomposites: research and commercial development. Journal of nanoscience and nanotechnology, 5(10), 1574-1592.

Zhou, Y., Goossens, J. G., Sijbesma, R. P., & Heuts, J. P. (2017). Poly (butylene terephthalate)/glycerol-based vitrimers via solid-state polymerization. Macromolecules, 50(17), 6742.